# Testing inferences from palaeocurrents

application of zircon double-dating to Miocene sediments from the Hengchun Peninsula, Taiwan

Cite As: Kirstein, LA, Carter, A & Chen, Y-G 2010, 'Testing inferences from palaeocurrents: application of zircon double-dating to Miocene sediments from the Hengchun Peninsula, Taiwan' *Terra nova*, vol 22, no. 6, pp. 483-493.

# Testing inferences from palaeocurrents: Application of zircon double-dating to Miocene sediments from the Hengchun Peninsula, Taiwan

Linda A. Kirstein[1], Andrew Carter[2] and Yue-Gau Chen[3]

[1]School of GeoSciences, University of Edinburgh, West Mains Road, Edinburgh EH9 3JW (linda.kirstein@ed.ac.uk)

[2]School of Earth Sciences, Birkbeck College, University of London, London, WC1E 7HX, U.K. (a.carter@ucl.ac.uk)

[3]Department of Geosciences, National Taiwan University, No.1, sec. 4th, Roosevelt Road, Taipei 10617, Taiwan, ROC. (ygchen@ntu.edu.tw)

## ABSTRACT

Detrital zircon provenance studies that combine low-temperature fission-track and high-temperature U-Pb single-grain age dating are powerful in constraining sediment provenance by documenting the tectono-thermal evolution of the sediment source(s). We apply these techniques to Miocene (12-6 Ma) sandstones of the Hengchun Peninsula, southern Taiwan which, based on diametrically opposite palaeocurrents, have a controversial provenance. U-Pb grain ages range from Miocene (8 Ma) to Archaean (2.5 Ga). Cretaceous thermal cooling is recorded by detrital zircon fission-tracks at Loshui and Lilongshan. Permian fission-track grain ages account for <33% of zircon ages from Loshui, while at Lilongshan Jurassic/Triassic grain ages account for 33-66% of all zircon fission-track ages. Minor (<12%) Miocene age components are detected in both formations. These new data suggest that the primary source of these Miocene sediments was similar. A simple model is proposed invoking sediment reworking in this complex tectonic setting.

## Introduction and Rationale

Sandstone palaeocurrents are widely used to infer different sediment source areas but this is rarely tested. A case in point is on Taiwan where Miocene sandstones of the Hengchun Peninsula show highly variable palaeocurrent directions (Sung & Wang, 1986). These have been interpreted as transportation from the north-northwest, from the south-southeast and from west to east (Cheng et al., 1984; Sung & Wang, 1986; Chang et al., 2003). Previous proposals to explain the palaeocurrent data have ignored complex currents in the depositional environment and suggest either an exotic source of sediment to the south (e.g. Sung & Wang, 1986) or that one of the units (Loshui) has been rotated during emplacement (e.g. Chang et al., 2003). These sandstones form part of the developing accretionary wedge and it is widely known that the composition of accretionary wedge sandstones can be affected by plate tectonic processes juxtaposing terranes, by magmatic arc dissection, by local structure and by recycling of sediment in the accretionary complex (e.g. Critelli, 1993). In these active tectonic settings, which are commonly characterized by elongated basins along orogenic strike, currents may be repeatedly changing and deflected or reflected by submarine topography. As a result, the use of palaeocurrents from these sediments to reconstruct for example, tectonic rotation (e.g. Chang et al., 2003), can be misleading.

To highlight the importance of reconstructing palaeodrainage not just by palaeocurrent direction we characterise the source formation age structure and post-metamorphic exhumation history. Zircon is a relatively ubiquitous, robust detrital mineral that can be double dated using fission-track and U-Pb dating techniques. It has been widely applied to successfully discriminate between source area contributions and unravel hinterland evolution (Carter & Moss, 1999). To test whether the palaeocurrent data have any real significance in the dynamic environment of an evolving accretionary complex and to resolve debate as to the origin of the sandstone material we applied detrital zircon dating techniques to Miocene sandstones of the Hengchun Peninsula, southern Taiwan in which highly variable palaeocurrent directions have been measured (Sung & Wang, 1986).

## Taiwan

The island of Taiwan is located at the boundary between the Eurasia Plate and the Philippine Sea Plate (PSP) (Figure 1). Subduction along the Manila Trench was initiated in the Oligocene/Miocene. The 4 km high Central Range of Taiwan, result from collision of the Luzon volcanic arc and South China continental margin since late Miocene – early

Pliocene times (Teng, 1987; Kirstein et al., 2010). The Hengchun Peninsula, southern Taiwan and offshore Hengchun Ridge form the present day accretionary prism, with accretionary wedge growth occurring both by frontal accretion, with sediments from the continental margin scraped up into the accretionary wedge (Liu et al., 2004), and by underplating (Fuller et al., 2006). Modern sands offshore southern Taiwan are lithic-rich and dominated by distinct geographic sources including the accretionary wedge, the Taiwan suture zone and the Luzon forearc basin (Yen & Lundberg, 2006). Deep sea canyons and channels together with submarine topography associated with subduction and collision influence sediment routing.

**Miocene Formations Hengchun Peninsula**

The Hengchun Peninsula includes the narrow southern-most segment of the Central Range and forms the southern tip of Taiwan (Figure 1). The lithologies include metamorphosed Miocene rocks with subordinate Pliocene sediments (Figure 2). The stratigraphy in the Hengchun region is complex and a number of stratigraphic schemes exist (e.g. Sung, 1991; Ho, 1999; Huang et al., 2006), here we combine the stratigraphy of Ho (1999) for the oldest formation with that of Huang et al. (2006) (Figure 2). The metamorphosed early Miocene Lushan Formation is the southwards extension of the Central Range (Ho, 1999) (Figure 1) and is structurally overlain by the middle to late Miocene Loshui and Mutan Formations (Huang et al., 2006).

Compositionally the mid Miocene Loshui (Loshui Formation) and mid/late Miocene Lilongshan sandstones (Mutan Formation) differ (Cheng et al., 1984) (Figure 2). The 1000 m thick Loshui sandstones generally contain less lithic grains and more quartz than the Lilongshan sandstones (Figure 2). Loshui grains are sub-angular to sub-rounded and quartz-rich, with locally high organic matter content (Figure 2). Igneous clasts vary in composition from andesite to rhyolite/granite. Loshui sandstones are classed as sub-arkosic arenites. Lilongshan sandstones are lithic arenites, rich in volcanic, sedimentary and meta-sedimentary lithic fragments (Figure 2). Several volcanic lithic fragments show textures consistent with rapidly quenched mafic lavas. Other fragments are silicic with feldspar phenocrysts in a cryptocrystalline matrix. Quartz, plagioclase, hornblende and calcite grains are evident, along with a number of fossil fragments. Chlorite has pseudomorphed volcanic glass although the original form is preserved. Combining the petrography and the available palaeocurrent directions, which in the Lilongshan sandstones are from the northwest and in

the Loshui sandstones from the southeast led some authors to propose (Cheng et al., 1984; Sung & Wang, 1986; Yen, 2003), distinct origins for these sandstones.

To test for distinct sources, samples were collected from key localities of Loshui and Lilongshan sandstones (Figure 2) and, where possible, zircon grains were double dated using a combination of low-temperature fission-track and higher temperature U-Pb dating methods (see Supplementary material A for details). The selected Loshui sandstones were medium to coarse-grained and deposited in mid Miocene times (~ 10-12 Ma; Sung, 1991). Sample LS3 was from the lower part of the sequence with obvious sedimentary structures. Sample LS1 was from the massive, upper part of the sequence. At Lilongshan, the sandstones were medium to course-grained with rounded to sub-angular mafic clasts. Sample LL1 is stratigraphically younger than sample LL2. Deposition of Lilongshan sandstones occurred between 11 and 6 Ma (Huang et al., 2006).

Previous thermochronology studies of Miocene sediments from the Hengchun Peninsula are limited by a lack of zircon in the samples. Where fission-track analyses of detrital zircons have been provided the number of grains analysed was < 10 or not reported (Yen, 2003; Huang et al., 2008) as a result data deconvolution to identify principal sources is not possible although Miocene and Cretaceous peak components were reported by Huang et al. (2008). To constrain potential sources more grain measurements are required. In addition, by coupling zircon fission-track (ZFT) and U-Pb dating techniques with petrology, the provenance can be further constrained by comparing formation ages with post metamorphic cooling histories.

**Results**

ZFT age data are reported in Tables 1 & 2, supplementary material DR Table 1 and Figure 3. Significant variance in single grain ages i.e. mixed age populations (Galbraith & Laslett, 1993) was detected in all samples. Deconvolution into grain-age populations was performed using the Binomfit program (Brandon, 1992). All samples have at least two significant grain-age populations (Table 2, Figure 3). At Loshui the majority of zircon grains (>60%) generate a Cretaceous peak component (Figure 3). LS3 from the base of the section has minor peaks in the Permian and Palaeocene, while LS1 also records input from a source with a Miocene cooling history (Table 2, Figure 3). Lilongshan sandstones record Miocene, Cretaceous, Jurassic and Triassic age components, with both samples dominated by Mesozoic grains (>85%; Table 2). In general ZFT grain ages from the Loshui and Lilongshan sandstones are remarkably similar and are dominated by grains which show

Cretaceous cooling. All ZFT grain ages are < 400 Ma with cooling ages as young as Late Miocene determined (Figure 3).

U-Pb dating of the same grains used for ZFT analysis yield crystallisation ages from Miocene through to Archaean (Table 1, Supplementary material Table DR2, Figure 4). U-Pb grain ages are not reported where the discordance between the uncorrected $^{206}Pb/^{238}U$ and $^{207}Pb/^{235}U$ ages was >10% (Table 1). The majority of the U-Pb grain age populations record formation events throughout the Mesozoic and Late Palaeozoic (110 – 360 Ma), Early Palaeozoic (460 – 520 Ma), Proterozoic (750 – 980 Ma; 1600 – 1990 Ma) and Late Archaean (<2790 Ma), with some Miocene age grains (Table 1, Figure 4). >35% of the grains are Cambrian or older, while at Loshui ~30% of the grains have Cretaceous U-Pb ages (Table 1). All samples have some concordant ZFT and U-Pb ages, particularly from the Cretaceous and Miocene (Figure 4).

**Discussion**

South China margin

The geology of southeast China in particular the South China Block (SCB) which consists of the Yangtze Craton and Cathaysia (Figure 5) is dominated by a wide Mesozoic magmatic belt with intense igneous activity in the Jurassic and Cretaceous (Wong et al., 2009). Late Permian – Triassic granites are widespread in the SCB (Wang et al., 2005) (Figure 5). As a result of these tectono-thermal events a spectrum of zircon crystallisation and cooling ages from Archaean to Cretaceous are anticipated from southeast China, with major crust building events listed in Table 3.

Concordant zircon FT and U-Pb ages between 260-125 Ma and 19-8 Ma record rapidly cooled magmatic sources (Figure 4) consistent with observed pebbles of basalt, andesite, gabbro and granodiorites in the sediments (this study, Pelletier & Stephan, 1986). Potential magmatic sources, outside mainland China are listed in Table 4, including the Luzon arc, Penghu Islands, intraplate magmatism and also oceanic lithosphere from the South China Sea and PSP. Early Cretaceous (Late Yenshanian) volcanism was widespread along the Chinese margin (Figure 5). Cretaceous grains originate from either rapidly cooled sources along the Chinese margin/proto-Taiwan (Figure 5) or from locally eroding old oceanic crust. The Loshui sandstones, which have most concordant ZFT and U-Pb Cretaceous grain-age components, contain primarily volcanic (andesite/dacite/rhyolite) lithic fragments. Early Cretaceous oceanic crust (131 – 119 Ma) is documented in the Huatung Basin and so erosion of the leading edge of the PSP cannot be discounted as a potential

source. Neogene intraplate magmatism in northwestern Taiwan occurred in the Early Miocene and Late Miocene (Table 4). The associated lithologies are basaltic and are not known to be zircon-bearing. South China Sea crust formed between 32 and 17 Ma and so cannot be the source of the young zircon grain-age component. Only the Luzon arc, which was initiated in the early Oligocene has zircon-bearing lithologies that crystallised during the necessary time interval.

Similar ZFT peak age components in the Miocene and Cretaceous are identified at Loshui and Lilongshan which suggests a similar tectono-thermal evolution for the grains. Older Permian ZFT peak age components were only detected at Loshui. These grains primarily have crystallisation ages that are Caledonian (c. 450-400 Ma) or older (Figure 4) and so may have cooled during subduction of the palaeo-Pacific Plate beneath South China in the Permian- Jurassic (Wong et al., 2009). Triassic and Jurassic ZFT grain-ages measured from Lilongshan have a similar range in crystallisation ages which suggests that no discrete, separate source region to the south need be invoked. However, the contribution of different sources varies with time, for example the Lilongshan sandstones have glassy magmatic fragments that have not travelled far since their original formation (Figure 2). These glassy fragments may well be sourced from the Penghu Islands but are not evident in the zircon analyses as the basaltic source rocks are not zircon bearing. The approach of coupling petrology with double dating of zircons from the detrital record highlights the importance of sediment recycling in this dynamic environment.

## Depositional environment

The Hengchun Peninsula is today one of the principal morpho-tectonic units in the domain of incipient continental subduction, while the region of oceanic subduction is located south of 21°N (Malavieille & Trullenque, 2009). Turbidite deposition of sand-rich units directed along sub-marine canyons and channels into a complex system of basins is documented on both sides of the accretionary prism (Lundberg et al., 1992). Petrology and thermochronology data from the preserved sediment pile in the Hengchun Peninsula indicate that an equally complex sediment routing system may have operated in the Miocene during the progression from oceanic subduction to ocean-continent subduction, pre arc-continent collision. The Chinese continental margin, local magmatic centres and oceanic crust were potentially significant sediment sources (Figure 6). The majority of the U-Pb and ZFT grain-age distributions from Loshui and Lilongshan suggest sediment was originally sourced from southeast China. The origin of the Cretaceous grain-age component is debatable but the

occurrence of gabbroic clasts argues in favour of some localised erosion of the leading edge of the PSP, and is consistent with analogue modelling (Malavieille & Trullenque, 2009). Miocene grain-age components from Loshui and Lilongshan can only be sourced from the Luzon arc. This suggests that sediment from the forearc region was incorporated and mixed with sediment from the continental margin as collision progressed in the Miocene. In the North Luzon Trough sediment sourced from the rear slope of the accretionary prism is combined with forearc derived sediments (Yen & Lundberg, 2006) indicating the potential for localised mixing. While modern canyon systems, such as the Penghu Canyon, erode both the continental margin and accretionary wedge (Liu et al., 2004). In this complex submarine environment, topography, slope stability and channelling of sediment are constantly changing generating complex palaeocurrent directions. Such a dynamic environment facilitates localised reworking and mixing of sediment and highlights the potential for sediment reworking and mixing within marginal accretionary prism environments in the past.

**Conclusions**

Miocene sandstones preserved in the Hengchun Peninsula, southern Taiwan were sourced locally from the Chinese continental margin, proto-Taiwan, magmatic centres (Penghu Islands; Luzon arc) and oceanic lithosphere. The majority of the zircon grains preserve U-Pb ages consistent with original source material from southeast China. ZFT grain-age components are related to major tectonic events in the SCB, connected to subduction of the palaeo-Pacific Plate. Significantly the ZFT ages, together with the petrography, suggest that the Luzon arc and leading edge of the PSP were actively eroding in the Miocene.

Loshui sandstones have not been rotated through 180 ° as previously proposed (Chang et al., 2003) nor do they originate from an exotic terrane to the south (e.g. Yen, 2003). Instead sediment deposition in the Miocene was strongly controlled by structural trends, crustal deformation and erosion in and around the developing accretionary prism. The different palaeocurrent directions preserved in the Loshui and Lilongshan sandstones reflect reworking of sediment in this chaotic environment. Similar structural controls occur in the modern offshore region today (e.g. Lundberg et al., 1997) and along other active margins.

**Acknowledgements**

The editor, associate editor, S. Critelli and three anonymous reviewers are thanked for constructive comments. This work was supported by NERC grant NE/E012426/1.

**References**

Brandon, M.T., 1992. Decomposition of fission-track grain-age distributions. *Amer. Jour. Sci.*, **292**, 535-564.

Carter, A. and Moss, S.J., 1999. Combined detrital-zircon fission-track and U-Pb dating: A new approach to understanding hinterland evolution. *Geology*, **27**, 235-238.

Chang C.-P., Angelier J.; Lee T.-Q., and Huang C.-Y., 2003. From continental margin extension to collision orogen: structural development and tectonic rotation of the Hengchun peninsula, southern Taiwan. *Tectonophysics*, **361**, 61-82.

Chen, C. H., Chung, S.-H., Hwang, H.-H., Chen, C.-H., and Chung, S.-L., 2001. Petrology and Geochemistry of Neogene Continental Basalts and Related Rocks in Northern Taiwan(III): Alkali Basalts and Tholeiites from Shiting-Yinko Area. *West. Pac. Earth Sci*., **19**, 19-46.

Cheng, Y.-M., Huang, C-Y., Yeh, J-J., and Chen, W-S., 1984. The Loshui Formation: Deeper-water sandstones on the Hengchun Peninsula, southern Taiwan. *Acta Geol. Taiwan.*, **22**, 100-117.

Chung, S-L., Yang, F.T., Lee, C-Y., and Chen, C-H., 1995. The igneous provinciality in Taiwan: consequence of continental rifting superimposed by Luzon and Ryukyu subduction systems. *Jour. South. Asian Earth Sci.*, **11**, 73-80.

Critelli, S., 1993. Sandstone detrital modes in the Paleogene Liguride Complex, accretionary wedge of the Southern Apennines (Italy). *Jour. Sed. Petrol*., **63**, 464-476.

Deschamps, A., Monié, P., Lallemand, S., Hsu, S.K., and Yeh, K.Y., 2000. Evidence for Early Cretaceous oceanic crust trapped in the Philippine Sea Plate. *Earth Planet. Sci. Letts*., **179**, 503-516.

Dickinson, W.R., 1985. Interpreting provenance relations from detrital modes of sandstones. In: Provenance of Arenites, G.G. Zuffa, Ed., NATO ASI Series, **148**, 333–361.

Fuller, C.W., Willett, S.D., Fisher, D., and Lu, C.-Y., 2006. A thermomechanical wedge model of Taiwan constrained by fission-track thermochronometry. *Tectonophysics,* **425,** 1–24.

Galbraith, R.F., and Laslett, G.M., 1993. Statistical models for mixed fission track ages. *Nucl. Tracks Rad. Meas.*, **21**, 459-470.

Ho, C.-S., 1999. An introduction to the geology of Taiwan: Taiwan, Central Geological Survey, 192 p.

Hsu, S.K., Yeh, Y., Doo, W.B., and Tsai, C.H. , 2004. New bathymetry and magnetic lineations identifications in the Northernmost South China Sea and their tectonic implications. *Mar. Geophys. Res*., **25**, 29-44.

Huang, C.Y., Yuan, P.B., and Tsao, S.H., 2006. Temporal and spatial records of active arc-continent collision in Taiwan: A synthesis. *Geol. Soc. Am. Bull*., **118**, 274–288.

Huang, C.-Y., Chien, C-W., Yao, B., and Chang, C-P., 2008. The Lichi Mélange: A collision mélange formation along early arcward backthrusts during forearc basin closure, Taiwan arc-continent collision. In: Draut, A.E., Clift, P.D., Scholl, D.W., ed., Formation and Applications of the Sedimentary Record in Arc Collision Zones, *Geol. Soc. Am. Spec. Paper*, **436**, 127-154.

Jahn, B.M., Zhou, X.H., and Li, J.L., 1990. Formation and tectonic evolution of Southeastern China and Taiwan: Isotopic and geochemical constraints. *Tectonophysics*, **183**, 145-160.

Kirstein, L.A., Fellin, M.G, Willett, S.D, Carter, A.C, Chen, Y-G, and Lee, D-C., 2010. Onset of rapid erosion in Taiwan during the Late Pliocene constrained by detrital thermochronology. *Basin Res*., **22**, 270-285 doi: 10.1111/j.1365-2117.2009.00426.x.

Liu, C.-S., Huang, I.L. and Teng, L.S., 1997. Structural features off southwestern Taiwan. *Mar. Geol.*, **137**, 305-319.

Liu, C.-S., Deffontaines, B., Lu, C-Y. and Lallemand, S., 2004. Deformation patterns of an accretionary wedge in the transition zone from subduction to collision offshore southwestern Taiwan. *Mar. Geophys. Res*., **25**, 123-137.

Lundberg, N., Reed, D.L., Liu, C.-S. and Lieske, J., 1997. Forearc-basin closure and arc accretion in the submarine suture zone south of Taiwan. *Tectonophysics*, **274**, 5-23.

Malavieille, J. and Trullenque, G., 2009. Consequences of continental subduction on forearc basin and accretionary wedge deformation in SE Taiwan: Insights from analogue modelling. *Tectonophysics*, **466**, 377-394.

Pelletier, B. and Stephan, J.F., 1986. Middle Miocene obduction and late Miocene beginning of collision registered in the Hengchun Peninsula: Geodynamic implications for the evolution of Taiwan. *Tectonophysics*, **125**, 133-160.

Richard, M., Bellon, H., Maury, R., Barrier, E. and Wen-Shing, J., 1986. Miocene to recent calc-alkalic volcanism in eastern Taiwan: K-Ar ages and petrography. *Tectonophysics*, **125**, 87-102.

Sung, Q., 1991. Explanatory text of the geological map of Taiwan, Hengchun Peninsula. Central Geological Survey, MOEA, 1-61.

Sung, Q. and Wang, Y., 1986. Sedimentary environments of the Miocene sediments in the Hengchun Peninsula and their tectonic implications. *Mem. Geol. Soc. China*, **7**, 325-340.

Teng, L.S., 1987. Tectonostratigraphic facies and geologic evolution of the Coastal Range, eastern Taiwan. *Mem. Geol. Soc. China*, **8**, 229-250.

Wang Q., Li J.-W., Jian P., Zhao Z.-H., Xiong X.-L., Bao Z.-W., Xu J.-F., Li C.-F., and Ma J.-L., 2005. Alkaline syenites in eastern Cathaysia (South China): link to Permian-Triassic transtension. *Earth Planet. Sci. Letts*., **230**, 339-354.

Wong J., Sun M., Xing G., Li X.-h., Zhao G., Wong K., Yuan C., Xia X., Li L., and Wu F., 2009. Geochemical and zircon U-Pb and Hf isotopic study of the Baijuhuajian metaluminous A-type granite: Extension at 125-100 Ma and its tectonic significance for South China. *Lithos*, **112**, 289-305.

Yen, J.Y., 2003. Provenance of Miocene sedimentary sequences in the Hengchun Peninsula, southern Taiwan, and implications for the modern Taiwan orogen, Florida State University, 132 p.

Yen, J.-Y. and Lundberg, N., 2006. Sediment compositions in offshore southern Taiwan and their relations to the source rocks in modern arc-continent collision zone: *Mar. Geol.,* **225**, 247-263.

Yu, S.-B., Chen, H-Y. and Kuo, L-C., 1997. Velocity field of GPS stations in the Taiwan area. *Tectonophysics*, **274**, 41-59.

Yu, H.-S. and Song, G-S., 1993. Submarine physiography around Taiwan and it's relation to tectonic setting. *Jour. Geol. Soc. China*, **36**, 139-156.

## Figures

**Figure 1.** Generalised tectonic and stratigraphic map of Taiwan with, from west to east, the geological divisions include: the Coastal Plain (CP), Western Foothills (WF), Central Range (Hsuehshan Range (HR), Backbone Slates (BS) & Tananao Complex (TC)), Longitudinal Valley (LV) and Coastal Range (CoR). Hengchun Peninsula (HP), volcanic rocks in the north-west (V). Submarine topography offshore of southern Taiwan includes a number of north-south trending submarine ridges and troughs (Hengchun Ridge; Southern Longitudinal Trough (SLT); Huatung Ridge; Taitung Trough (TT); Lutao-Lanshu Ridge) (Yu & Song, 1993; Huang et al., 2006). Each of these large scale features has highly variable internal topography which influences sediment routing. Inset shows direction of plate motion from Yu et al. (1997) and position of Philippine Sea Plate relative to Eurasia and location of the Luzon arc.

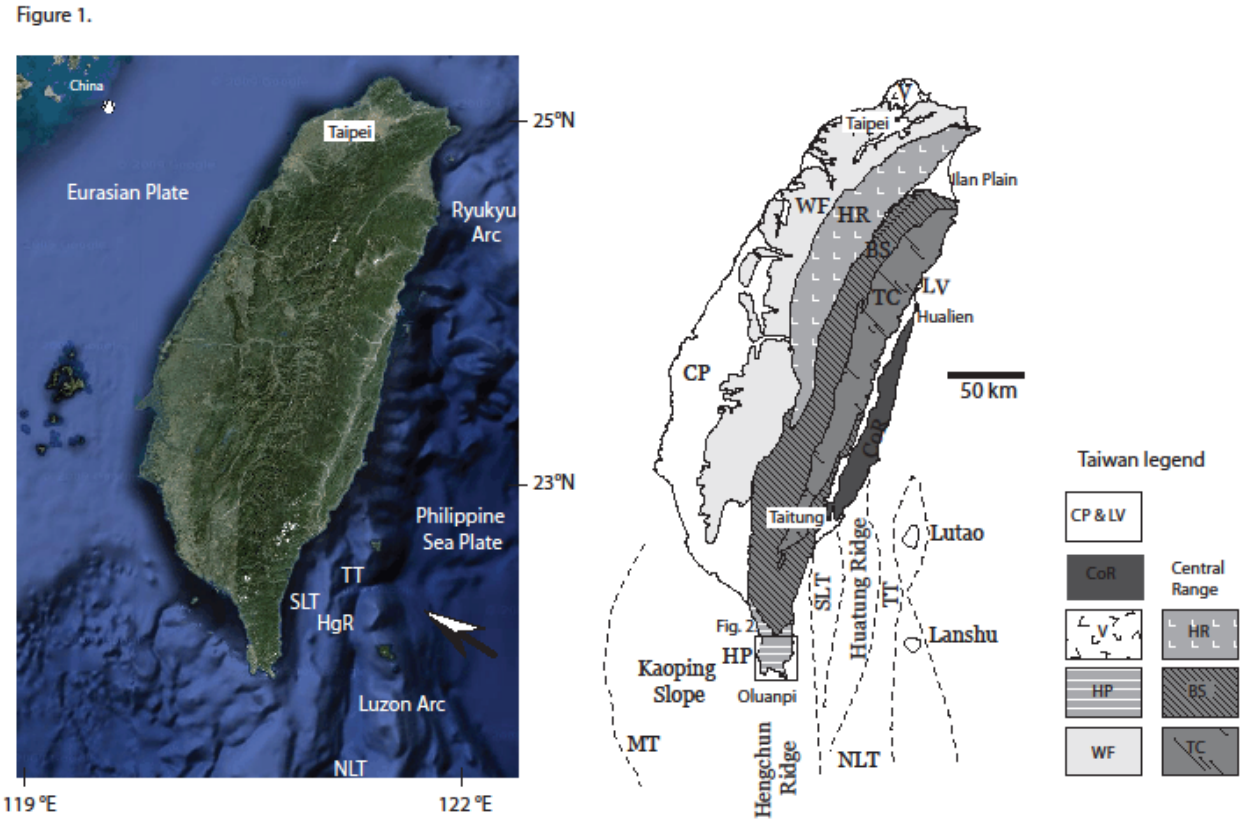

**Figure 2**. Enlarged map of part of the Hengchun Peninsula in which mid to late Miocene sandstones crop out, after Huang et al. (2006). Black squares sample sites for fission-track and U-Pb analyses. Mutan Formation includes the Lilongshan sandstones. Inset photomicrographs show Lilongshan lithic arenites ( LL1) and Loshui sub-arkosic arenites (LS1). Quartz (q), plagioclase feldspar (p), alkali feldspar (a), volcanic lithics (v), meta-sedimentary lithics (s), volcanic glass (g), muscovite (m), calcite (c), amphibole (h). Palaeocurrent data from Cheng et al. (1984); Sung & Wang (1986) and Yen (2003). Quartz-feldspar-lithic ternary diagram after Dickinson (1985) illustrates lithic-rich nature of Lilongshan sandstones versus quartz-rich Loshui sandstones. Data from Sung & Wang (1986); this study.

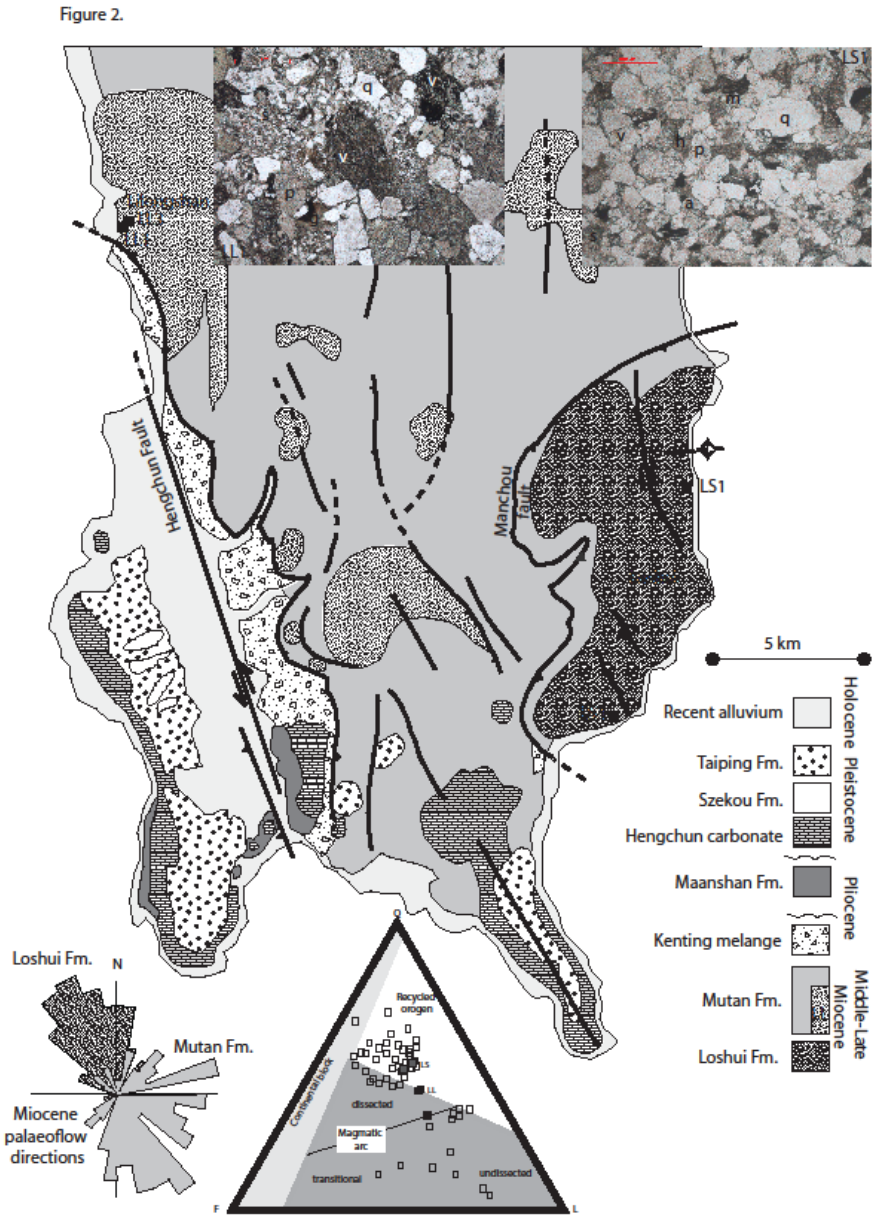

**Figure 3.** Detrital zircon fission-track grain age distributions from measured samples highlighting significant Cretaceous peaks. Samples LS from Loshui; LL from Lilongshan. Other peak age components range from Miocene through to Permian. Inset shows U-Pb grain age distributions which range from Miocene through to Archaean. Depositional age constraints from Sung (1991) and Huang et al. (2006).

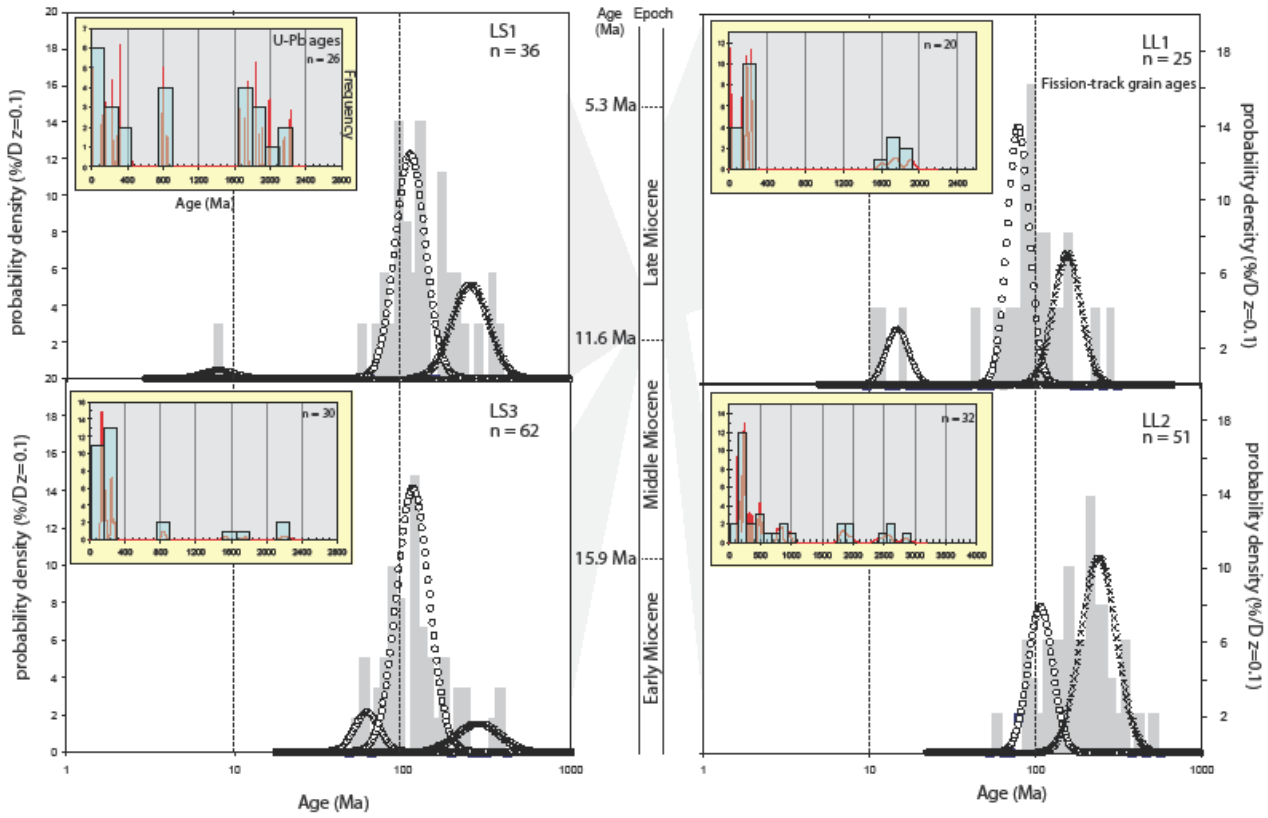


Figure 3.

**Figure 4.** Plot of zircon fission-track versus $^{238}U$-$^{206}Pb$ grain ages for all samples analysed highlighting the sources of the grains dated. Major crust forming events affecting SE China labelled indicating that the majority of grains were originally sourced from southeast China. Dashed line shows concordant ZFT and U-Pb ages indicating rapidly cooled magmatic sources. Open diamonds LS3; filled diamonds LS1; open squares LL1; filled squares LL2.

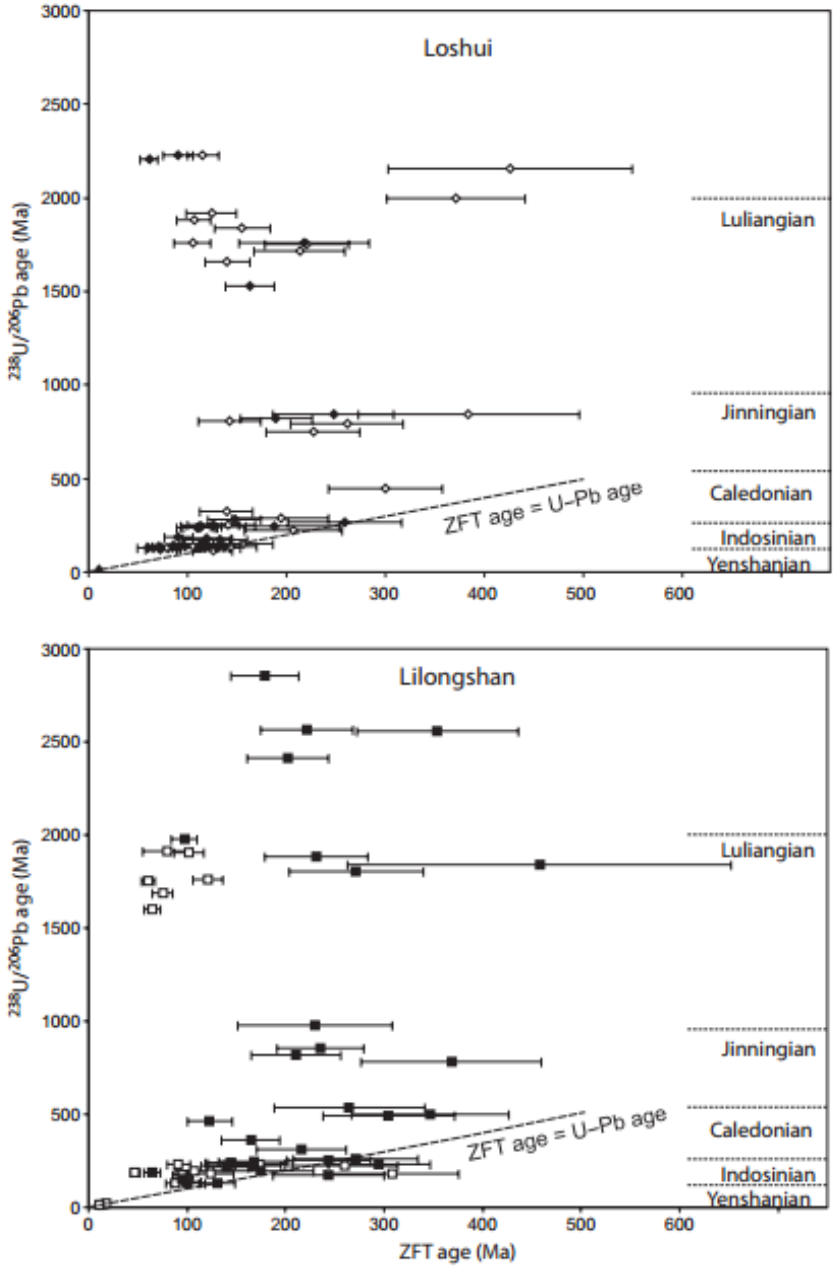

**Figure 5.** Schematic map of SE China showing the distribution of late Palaeozoic and Mesozoic intrusive and extrusive magmatic rocks after Wong et al. (2009); Wang et al. (2005). SCB = South China Block which includes both Cathaysia and Yangtze Craton basement.

Figure 5.

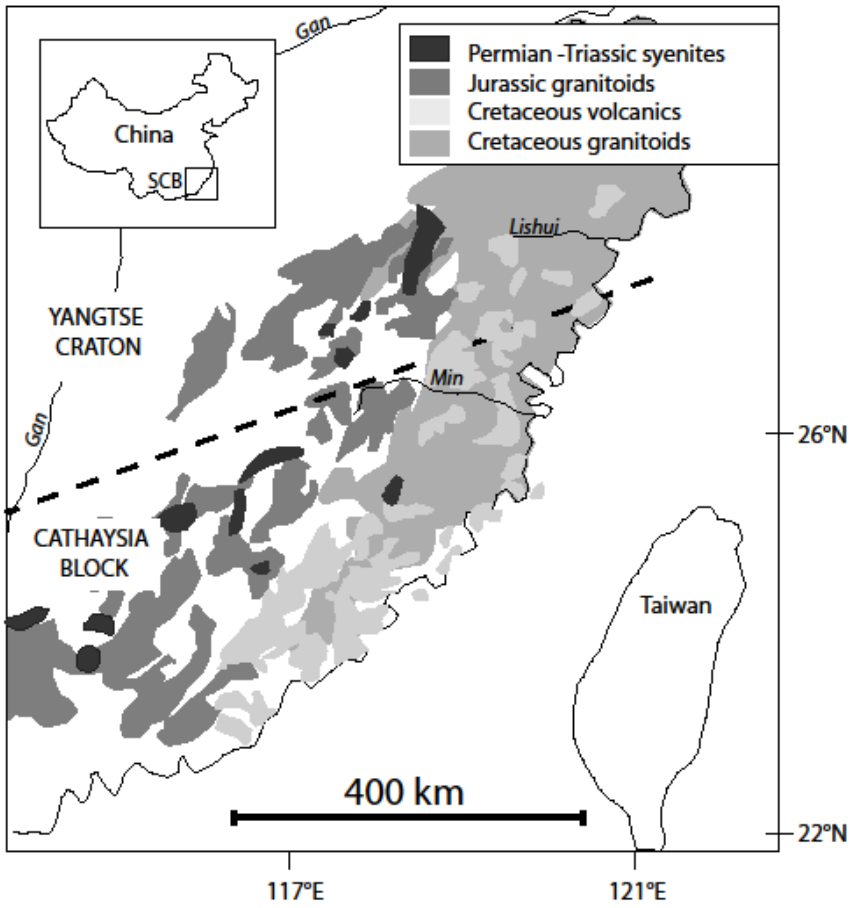

**Figure 6.** Reconstruction of the tectonic evolution of Taiwan at key stages during the deposition of the Hengchun Miocene sandstone units after Chung et al. (1995). Double-ended arrows indicate regions of extension. CSB – continental shelf break; BOS – base of slope; P – Penghu Islands intraplate magmatism; EP – Eurasian Plate; PSP – Philippine Sea Plate; LA – Luzon Arc; RT – Ryukyu Trench; MT – Manila Trench. Arrows indicate sediment pathways. Plate motion after Yu et al. (1987).

Figure 6.

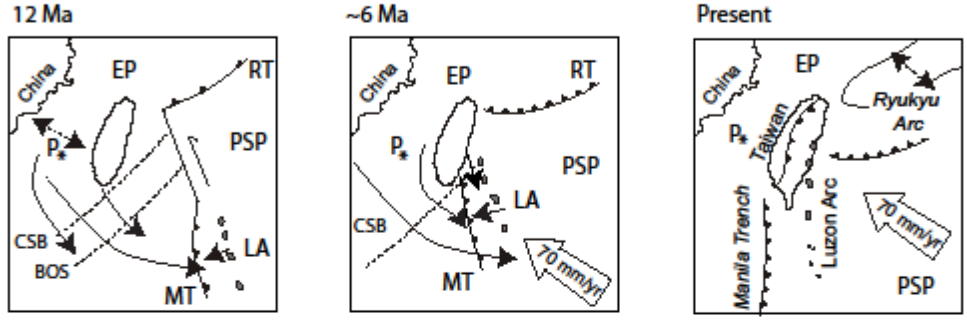

Table 1. Results from double-dating zircon grains using fission-track and U-Pb dating techniques.

| Sample | crystal | Ns | Ni | U (ppm) | FT age (Ma) | ± | Uncorrected ages (Ma) $^{206}Pb/^{238}U$ | ± 2σ | $^{207}Pb/^{235}U$ | ± 2σ | $^{207}Pb/^{206}Pb$ | ± 2σ | % discordance |
|---|---|---|---|---|---|---|---|---|---|---|---|---|---|
| LS1 | 1 | 244 | 31 | 177 | 300 | 57 | 446.2 | 4.3 | 444.1 | 23.3 | 626.1 | 30.5 | -0.5 |
| | 2 | 153 | 38 | 290 | 155 | 28 | 1839.3 | 0.8 | 1849.7 | 107.1 | 1855.2 | 11.5 | 0.6 |
| | 3 | 150 | 58 | 332 | 100 | 16 | | | | | | | |
| | 4 | 80 | 16 | 122 | 192 | 53 | | | | | | | |
| | 5 | 98 | 48 | 183 | 79 | 14 | 127.5 | 1.7 | 138.3 | 8.3 | 408.6 | 47.9 | 7.8 |
| | 6 | 147 | 13 | 99 | 427 | 124 | 2156.7 | 3.0 | 2113.9 | 409.0 | 2260.8 | 17.2 | -2.0 |
| | 7 | 138 | 60 | 275 | 89 | 14 | | | | | | | |
| | 8 | 182 | 50 | 286 | 140 | 23 | 1658.2 | 1.5 | 1735.0 | 91.6 | 1870.6 | 11.5 | 4.4 |
| | 9 | 43 | 27 | 155 | 62 | 15 | | | | | | | |
| | 10 | 149 | 54 | 412 | 107 | 17 | 1879.8 | 2.7 | 1911.9 | 132.1 | 2024.8 | 11.6 | 1.7 |
| | 11 | 304 | 31 | 118 | 372 | 70 | 1994.2 | 1.3 | 1933.0 | 120.9 | 1917.2 | 11.4 | -3.2 |
| | 12 | 184 | 32 | 122 | 221 | 42 | 1751.2 | 1.5 | 1778.3 | 107.6 | 1846.9 | 11.8 | 1.5 |
| | 13 | 164 | 24 | 137 | 261 | 57 | 792.5 | 1.6 | 786.8 | 32.2 | 819.6 | 17.8 | -0.7 |
| | 14 | 103 | 32 | 244 | 124 | 25 | 1916.8 | 2.2 | 1809.7 | 203.5 | 1883.6 | 14.8 | -5.9 |
| | 15 | 130 | 36 | 275 | 139 | 26 | 322.6 | 0.7 | 321.5 | 12.9 | 400.4 | 27.8 | -0.3 |
| | 16 | 111 | 59 | 270 | 73 | 12 | | | | | | | |
| | 17 | 160 | 27 | 155 | 227 | 47 | 750.8 | 1.3 | 741.6 | 32.8 | 836.8 | 19.1 | -1.2 |
| | 18 | 123 | 45 | 258 | 106 | 18 | | | | | | | |
| | 19 | 117 | 32 | 147 | 141 | 28 | 250.4 | 3.4 | 255.5 | 10.3 | 343.7 | 29.6 | 2.0 |
| | 20 | 82 | 40 | 305 | 79 | 15 | | | | | | | |
| | 21 | 106 | 41 | 313 | 100 | 18 | | | | | | | |
| | 22 | 139 | 25 | 143 | 213 | 46 | 1713.2 | 1.8 | 1629.9 | 126.5 | 1666.1 | 13.9 | -5.1 |
| | 23 | 31 | 149 | 682 | *8* | *2* | *7.2* | *0.9* | | | | | |
| | 24 | 96 | 26 | 149 | 142 | 32 | 805.9 | 0.7 | 850.5 | 53.6 | 1152.0 | 22.0 | 5.2 |
| | 25 | 224 | 75 | 343 | 115 | 16 | 2227.6 | 1.5 | 2231.6 | 147.0 | 2261.4 | 10.7 | 0.1 |
| | 26 | 130 | 35 | 160 | 143 | 27 | 135.1 | 0.7 | 130.6 | 7.7 | 163.5 | 49.0 | -3.5 |
| | 27 | 122 | 45 | 258 | 105 | 18 | 1758.3 | 1.0 | 1759.8 | 95.6 | 1841.3 | 11.6 | 0.1 |

| Sample | crystal | Ns | Ni | U (ppm) | FT age (Ma) | ± | Uncorrected ages (Ma) | | | | | | % |
|---|---|---|---|---|---|---|---|---|---|---|---|---|---|
| | | | | | | | $^{206}Pb/^{238}U$ | ± 2σ | $^{207}Pb/^{235}U$ | ± 2σ | $^{207}Pb/^{206}Pb$ | ± 2σ | discordance |
| | 28 | 134 | 33 | 151 | 157 | 31 | 149.4 | 1.2 | 155.1 | 8.6 | 356.8 | 44.8 | 3.7 |
| | 29 | 176 | 54 | 137 | 126 | 20 | 113.2 | 2.1 | 106.5 | 7.3 | 116.9 | 57.7 | -6.4 |
| | 30 | 90 | 33 | 189 | 106 | 22 | 138.2 | 0.9 | 148.5 | 8.9 | 357.6 | 48.5 | 6.9 |
| | 31 | 96 | 19 | 109 | 194 | 49 | 289.1 | 2.8 | 305.3 | 20.8 | 580.7 | 47.0 | 5.3 |
| | 32 | 132 | 13 | 74 | 384 | 112 | 846.1 | 2.8 | 828.5 | 44.7 | 943.2 | 20.5 | -2.1 |
| | 33 | 113 | 21 | 160 | 207 | 49 | 223.8 | 0.7 | 225.1 | 10.9 | 358.9 | 37.2 | 0.6 |
| | 34 | 69 | 24 | 137 | 111 | 26 | | | | | | | |
| | 35 | 116 | 24 | 183 | 186 | 42 | | | | | | | |
| | 36 | 113 | 24 | 137 | 181 | 41 | | | | | | | |
| LS3 | 1 | 96 | 42 | 160 | 89 | 16 | 127.5 | 5.6 | 123.8 | 11.0 | 138.7 | 82.4 | -2.9 |
| | 2 | 75 | 30 | 114 | 97 | 21 | 139.5 | 5.8 | 136.9 | 11.5 | 238.1 | 76.2 | -1.9 |
| | 3 | 110 | 45 | 294 | 95 | 17 | | | | | | | |
| | 4 | 105 | 33 | 189 | 123 | 25 | | | | | | | |
| | 5 | 131 | 56 | 427 | 91 | 15 | 2227.1 | 46.0 | 2314.6 | 138.8 | 2365.0 | 11.5 | 3.8 |
| | 6 | 180 | 65 | 298 | 107 | 16 | | | | | | | |
| | 7 | 61 | 24 | 110 | 98 | 24 | | | | | | | |
| | 8 | 163 | 33 | 189 | 190 | 36 | 823.6 | 16.9 | 825.6 | 49.5 | 919.2 | 23.5 | 0.2 |
| | 9 | 52 | 18 | 103 | 112 | 31 | 128.9 | 5.8 | 127.9 | 11.8 | 229.5 | 84.3 | -0.8 |
| | 10 | 145 | 43 | 246 | 130 | 23 | | | | | | | |
| | 11 | 109 | 35 | 200 | 120 | 23 | | | | | | | |
| | 12 | 94 | 32 | 163 | 114 | 23 | 136.0 | 5.7 | 151.6 | 11.7 | 469.7 | 66.0 | 10 |
| | 13 | 126 | 50 | 286 | 98 | 16 | | | | | | | |
| | 14 | 103 | 30 | 137 | 133 | 28 | 174.4 | 6.0 | 173.9 | 11.6 | 299.0 | 56.9 | -0.3 |
| | 15 | 147 | 30 | 229 | 188 | 38 | | | | | | | |
| | 16 | 74 | 13 | 99 | 218 | 66 | 1760.8 | 35.4 | 1686.8 | 122.7 | 1757.3 | 13.9 | -4.4 |
| | 17 | 153 | 40 | 153 | 148 | 26 | 278.2 | 7.3 | 256.6 | 14.4 | 276.1 | 44.0 | -8.4 |
| | 18 | 186 | 72 | 275 | 100 | 14 | | | | | | | |
| | 19 | 110 | 37 | 169 | 115 | 22 | | | | | | | |
| | 20 | 68 | 11 | 42 | 237 | 77 | | | | | | | |

| Sample | crystal | Ns | Ni | U (ppm) | FT age (Ma) | ± | Uncorrected ages (Ma) | | | | | | |
|---|---|---|---|---|---|---|---|---|---|---|---|---|---|
| | | | | | | | $^{206}Pb/^{238}U$ | ± 2σ | $^{207}Pb/^{235}U$ | ± 2σ | $^{207}Pb/^{206}Pb$ | ± 2σ | % discordance |
| | 21 | 64 | 34 | 195 | 73 | 16 | 120.8 | 5.3 | 121.7 | 8.8 | 341.6 | 61.3 | 0.7 |
| | 22 | 85 | 39 | 223 | 84 | 16 | | | | | | | |
| | 23 | 156 | 23 | 105 | 259 | 58 | 269.4 | 7.3 | 258.5 | 15.9 | 356.4 | 47.8 | -4.2 |
| | 24 | 139 | 46 | 211 | 117 | 20 | 141.2 | 5.4 | 142.6 | 7.6 | 257.5 | 41.0 | 1.0 |
| | 25 | 122 | 34 | 260 | 138 | 27 | 196.0 | 6.3 | 201.0 | 13.7 | 318.1 | 56.2 | 2.5 |
| | 26 | 68 | 23 | 59 | 114 | 28 | 150.0 | 6.3 | 146.7 | 15.3 | 396.5 | 95.8 | -2.3 |
| | 27 | 55 | 25 | 143 | 85 | 21 | 135.2 | 6.4 | 139.5 | 16.6 | 494.2 | 107.9 | 3.1 |
| | 28 | 93 | 30 | 172 | 120 | 25 | 174.3 | 5.8 | 176.9 | 9.7 | 306.4 | 44.1 | 1.4 |
| | 29 | 66 | 16 | 122 | 159 | 44 | | | | | | | |
| | 30 | 105 | 38 | 290 | 107 | 20 | | | | | | | |
| | 31 | 62 | 19 | 145 | 126 | 33 | 247.6 | 6.9 | 262.5 | 14.0 | 472.1 | 40.2 | 5.7 |
| | 32 | 99 | 32 | 244 | 120 | 24 | 178.9 | 5.8 | 196.8 | 9.4 | 503.5 | 36.0 | 9.1 |
| | 33 | 147 | 50 | 254 | 114 | 19 | | | | | | | |
| | 34 | 47 | 4 | 23 | 443 | 231 | | | | | | | |
| | 35 | 224 | 53 | 303 | 163 | 25 | 1530.9 | 31.0 | 1654.0 | 86.2 | 1854.9 | 13.5 | 7.4 |
| | 36 | 114 | 40 | 122 | 110 | 20 | | | | | | | |
| | 37 | 76 | 36 | 275 | 82 | 17 | | | | | | | |
| | 38 | 90 | 26 | 198 | 134 | 30 | | | | | | | |
| | 39 | 120 | 41 | 313 | 113 | 21 | 241.6 | 6.7 | 244.4 | 11.8 | 300.3 | 37.3 | 1.1 |
| | 40 | 129 | 55 | 315 | 91 | 15 | 184.4 | 5.8 | 185.6 | 8.1 | 267.7 | 32.8 | 0.6 |
| | 41 | 49 | 10 | 57 | 188 | 65 | 246.6 | 7.3 | 241.4 | 16.0 | 385.2 | 52.3 | -2.2 |
| | 42 | 101 | 31 | 142 | 126 | 26 | 252.0 | 7.5 | 253.2 | 17.9 | 377.7 | 55.4 | 0.5 |
| | 43 | 40 | 14 | 107 | 111 | 34 | | | | | | | |
| | 44 | 172 | 109 | 416 | 61 | 8 | | | | | | | |
| | 45 | 132 | 84 | 641 | 61 | 9 | 2203.4 | 46.7 | 2194.3 | 144.8 | 2216.7 | 12.8 | -1.4 |
| | 46 | 77 | 50 | 382 | 60 | 11 | 131.8 | 5.4 | 134.5 | 7.6 | 213.9 | 44.3 | 2.1 |
| | 47 | 123 | 19 | 109 | 248 | 61 | 846.0 | 17.7 | 785.0 | 43.7 | 804.8 | 23.9 | -7.8 |
| | 48 | 185 | 64 | 183 | 112 | 16 | 241.0 | 6.7 | 238.3 | 11.6 | 318.1 | 37.8 | -1.1 |
| | 49 | 102 | 39 | 298 | 101 | 19 | | | | | | | |

| Sample | crystal | Ns | Ni | U (ppm) | FT age (Ma) | ± | Uncorrected ages (Ma) | | | | | | |
|---|---|---|---|---|---|---|---|---|---|---|---|---|---|
| | | | | | | | $^{206}Pb/^{238}U$ | ± 2σ | $^{207}Pb/^{235}U$ | ± 2σ | $^{207}Pb/^{206}Pb$ | ± 2σ | % discordance |
| | 50 | 87 | 47 | 154 | 72 | 13 | 138.9 | 5.6 | 143.1 | 9.9 | 268.6 | 58.4 | 2.9 |
| | 51 | 57 | 24 | 183 | 92 | 22 | 133.9 | 5.5 | 137.9 | 8.9 | 321.5 | 53.1 | 2.9 |
| | 52 | 111 | 39 | 223 | 110 | 21 | 236.1 | 6.6 | 237.6 | 6.6 | 297.7 | 33.1 | 0.6 |
| | 53 | 90 | 25 | 191 | 139 | 31 | | | | | | | |
| | 54 | 199 | 49 | 224 | 157 | 25 | | | | | | | |
| | 55 | 301 | 29 | 111 | 393 | 77 | | | | | | | |
| | 56 | 86 | 29 | 190 | 115 | 25 | | | | | | | |
| | 57 | 47 | 18 | 137 | 101 | 28 | | | | | | | |
| | 58 | 118 | 36 | 275 | 127 | 24 | | | | | | | |
| | 59 | 129 | 42 | 192 | 119 | 21 | | | | | | | |
| | 60 | 156 | 113 | 518 | 54 | 7 | | | | | | | |
| | 61 | 64 | 6 | 46 | 403 | 172 | | | | | | | |
| | 62 | 99 | 34 | 260 | 113 | 22 | | | | | | | |
| LL1 | 1 | 145 | 40 | 305 | 140 | 25 | 226.1 | 5.4 | 234.5 | 8.5 | 306.8 | 28.8 | 3.6 |
| | 2 | 184 | 27 | 155 | 261 | 54 | 227.1 | 5.7 | 247.1 | 12.3 | 480.7 | 38.3 | 8.1 |
| | 3 | 45 | 136 | 623 | *13* | *2* | *12.2* | *3.3* | | | | | |
| | 4 | 119 | 37 | 188 | 124 | 23 | 183.4 | 4.9 | 187.0 | 8.6 | 199.6 | 39.1 | 1.9 |
| | 5 | 196 | 125 | 477 | 61 | 7 | 1755.6 | 34.9 | 1809.0 | 82.5 | 1881.5 | 11.4 | 3.0 |
| | 6 | 167 | 65 | 372 | 99 | 15 | 138.8 | 5.2 | 146.1 | 13.4 | 491.9 | 82.5 | 5.0 |
| | 7 | 118 | 45 | 206 | 102 | 18 | | | | | | | |
| | 8 | 161 | 83 | 380 | 75 | 10 | 1686.7 | 33.6 | 1772.3 | 82.7 | 1883.6 | 11.9 | 4.8 |
| | 9 | 166 | 99 | 453 | 65 | 8 | 1600.8 | 31.9 | 1716.4 | 85.5 | 1902.4 | 12.3 | 6.7 |
| | 10 | 246 | 108 | 412 | 88 | 10 | 133.7 | 4.4 | 147.5 | 8.6 | 465.4 | 50.1 | 9.3 |
| | 11 | 191 | 81 | 371 | 91 | 12 | 233.4 | 5.7 | 236.6 | 10.8 | 333.1 | 36.4 | 1.3 |
| | 12 | 262 | 58 | 266 | 174 | 25 | 232.0 | 5.7 | 249.2 | 11.8 | 462.2 | 36.4 | 6.9 |
| | 13 | 200 | 69 | 316 | 112 | 16 | | | | | | | |
| | 14 | 250 | 206 | 674 | 47 | 4 | 184.9 | 4.8 | 194.8 | 7.7 | 361.4 | 32.1 | 5.1 |
| | 15 | 152 | 34 | 156 | 172 | 33 | | | | | | | |
| | 16 | 130 | 289 | 662 | *18* | *2* | *18.9* | *3.3* | | | | | |

| Sample | crystal | Ns | Ni | U (ppm) | FT age (Ma) | ± | Uncorrected ages (Ma) | | | | | | |
|---|---|---|---|---|---|---|---|---|---|---|---|---|---|
| | | | | | | | $^{206}Pb/^{238}U$ | ± 2σ | $^{207}Pb/^{235}U$ | ± 2σ | $^{207}Pb/^{206}Pb$ | ± 2σ | % discordance |
| | 17 | 155 | 59 | 338 | 102 | 16 | 1906.9 | 39.5 | 1920.2 | 125.1 | 1967.3 | 12.8 | 0.7 |
| | 18 | 272 | 87 | 398 | 121 | 15 | 1758.3 | 36.0 | 1810.7 | 100.9 | 1873.3 | 13.0 | 2.9 |
| | 19 | 47 | 161 | 614 | *11* | *2* | *10.9* | *3.3* | *13.8* | *3.6* | | | |
| | 20 | 157 | 62 | 284 | 98 | 15 | | | | | | | |
| | 21 | 111 | 40 | 305 | 107 | 20 | 193.8 | 5.2 | 196.7 | 9.4 | 319.8 | 39.7 | 1.5 |
| | 22 | 134 | 35 | 200 | 148 | 28 | | | | | | | |
| | 23 | 186 | 23 | 88 | 308 | 68 | 178.5 | 5.0 | 180.3 | 9.2 | 343.3 | 43.0 | 1.0 |
| | 24 | 33 | 16 | 61 | 80 | 24 | 1912.1 | 41.5 | 1820.3 | 188.2 | 1891.0 | 16.0 | -5.0 |
| | 25 | 326 | 132 | 378 | 96 | 10 | 173.1 | 4.9 | 169.1 | 8.5 | 190.8 | 43.5 | -2.4 |
| LL2 | 1 | 191 | 76 | 435 | 97 | 13 | 1976.9 | 39.1 | 1794.9 | 182.4 | 1785.9 | 15.3 | -10 |
| | 2 | 97 | 14 | 107 | 265 | 76 | 537.3 | 10.5 | 521.2 | 25.7 | 580.3 | 27.3 | -3.1 |
| | 3 | 128 | 18 | 41 | 272 | 69 | 1806.8 | 34.9 | 1782.9 | 155.7 | 1809.5 | 14.8 | -1.3 |
| | 4 | 150 | 26 | 60 | 221 | 47 | 2567.9 | 52.9 | 2358.7 | 308.2 | 2345.4 | 13.7 | -8.9 |
| | 5 | 60 | 10 | 38 | 230 | 79 | 980.9 | 20.7 | 891.4 | 78.4 | 998.3 | 29.4 | -10 |
| | 6 | 286 | 37 | 141 | 295 | 52 | 230.2 | 5.9 | 227.6 | 12.0 | 242.2 | 41.3 | -1.2 |
| | 7 | 244 | 72 | 236 | 131 | 18 | 131.3 | 4.5 | 129.5 | 6.3 | 136.8 | 37.8 | -1.4 |
| | 8 | 124 | 39 | 223 | 123 | 23 | 462.6 | 9.2 | 451.7 | 18.3 | 456.7 | 25.2 | -2.4 |
| | 9 | 150 | 40 | 229 | 145 | 26 | 237.6 | 5.7 | 236.6 | 8.9 | 241.7 | 28.3 | -0.4 |
| | 10 | 137 | 25 | 114 | 210 | 46 | 817.9 | 15.7 | 760.6 | 37.6 | 762.3 | 22.2 | -7.5 |
| | 11 | 59 | 13 | 74 | 175 | 54 | 193.8 | 5.5 | 179.9 | 10.7 | 194.5 | 50.4 | -7.7 |
| | 12 | 152 | 27 | 124 | 216 | 45 | 313.8 | 7.3 | 296.1 | 16.3 | 312.4 | 40.4 | -6.0 |
| | 13 | 192 | 24 | 137 | 305 | 66 | 492.2 | 10.8 | 524.9 | 30.6 | 777.2 | 31.3 | 6.2 |
| | 14 | 169 | 70 | 401 | 94 | 13 | | | | | | | |
| | 15 | 170 | 80 | 458 | 82 | 11 | | | | | | | |
| | 16 | 149 | 21 | 192 | 271 | 63 | 259.4 | 6.8 | 263.8 | 13.7 | 328.4 | 39.6 | 1.7 |
| | 17 | 175 | 18 | 103 | 369 | 91 | 779.1 | 15.8 | 775.8 | 42.3 | 889.1 | 22.7 | 0.4 |
| | 18 | 157 | 43 | 197 | 141 | 24 | | | | | | | |
| | 19 | 158 | 34 | 156 | 179 | 34 | 2857.2 | 63.0 | 2790.0 | 386.8 | 2833.0 | 11.5 | -2.4 |
| | 20 | 74 | 23 | 176 | 124 | 30 | | | | | | | |

| Sample | crystal | Ns | Ni | U (ppm) | FT age (Ma) | ± | Uncorrected ages (Ma) | | | | | | |
|---|---|---|---|---|---|---|---|---|---|---|---|---|---|
| | | | | | | | $^{206}Pb/^{238}U$ | ± 2σ | $^{207}Pb/^{235}U$ | ± 2σ | $^{207}Pb/^{206}Pb$ | ± 2σ | % discordance |
| | 21 | 187 | 43 | 281 | 167 | 28 | 227.4 | 6.1 | 247.4 | 9.7 | 518.0 | 28.9 | 8.1 |
| | 22 | 62 | 14 | 128 | 171 | 51 | | | | | | | |
| | 23 | 175 | 31 | 237 | 217 | 42 | | | | | | | |
| | 24 | 153 | 29 | 133 | 203 | 41 | 2415.8 | 52.1 | 2328.0 | 261.6 | 2365.1 | 12.8 | -3.8 |
| | 25 | 237 | 45 | 147 | 202 | 33 | | | | | | | |
| | 26 | 139 | 23 | 176 | 232 | 52 | 1886.9 | 39.9 | 1863.3 | 170.3 | 1831.5 | 15.3 | -1.3 |
| | 27 | 150 | 53 | 347 | 109 | 18 | | | | | | | |
| | 28 | 135 | 35 | 267 | 149 | 28 | | | | | | | |
| | 29 | 192 | 21 | 160 | 347 | 80 | 498.0 | 10.5 | 474.1 | 21.4 | 477.9 | 27.6 | -5.0 |
| | 30 | 434 | 178 | 679 | 94 | 9 | 155.6 | 5.2 | 168.8 | 6.8 | 384.3 | 28.9 | 7.8 |
| | 31 | 125 | 48 | 244 | 101 | 17 | 132.6 | 5.2 | 134.6 | 9.2 | 245.8 | 59.2 | 1.5 |
| | 32 | 86 | 18 | 118 | 184 | 48 | | | | | | | |
| | 33 | 140 | 22 | 168 | 244 | 56 | 172.5 | 5.6 | 176.0 | 9.2 | 290.7 | 42.7 | 2.0 |
| | 34 | 73 | 6 | 34 | 458 | 195 | 1841.9 | 43.9 | 1742.0 | 266.1 | 1802.7 | 23.2 | -5.7 |
| | 35 | 177 | 30 | 137 | 226 | 45 | | | | | | | |
| | 36 | 183 | 110 | 630 | 65 | 8 | 187.5 | 5.6 | 188.1 | 7.6 | 171.1 | 31.0 | 0.3 |
| | 37 | 167 | 39 | 223 | 165 | 29 | 360.7 | 7.8 | 345.8 | 17.8 | 366.9 | 35.3 | -4.3 |
| | 38 | 179 | 28 | 128 | 245 | 50 | | | | | | | |
| | 39 | 187 | 50 | 229 | 144 | 23 | 240.1 | 6.4 | 240.1 | 10.5 | 287.2 | 33.7 | 0.0 |
| | 40 | 126 | 29 | 166 | 167 | 35 | 243.5 | 6.8 | 257.8 | 14.8 | 465.8 | 43.5 | 5.5 |
| | 41 | 130 | 41 | 313 | 123 | 22 | | | | | | | |
| | 42 | 229 | 32 | 147 | 273 | 52 | | | | | | | |
| | 43 | 196 | 21 | 160 | 354 | 82 | 2554.9 | 57.8 | 2525.5 | 290.6 | 2519.1 | 15.1 | -1.2 |
| | 44 | 242 | 38 | 218 | 244 | 43 | 251.2 | 6.6 | 258.9 | 11.2 | 358.9 | 32.6 | 3.0 |
| | 45 | 159 | 33 | 252 | 185 | 36 | | | | | | | |
| | 46 | 217 | 30 | 114 | 276 | 54 | | | | | | | |
| | 47 | 156 | 10 | 46 | 582 | 190 | | | | | | | |
| | 48 | 203 | 33 | 151 | 236 | 44 | 853.3 | 15.5 | 812.2 | 37.1 | 850.2 | 19.2 | -5.1 |
| | 49 | 201 | 55 | 252 | 141 | 22 | 215.7 | 5.4 | 234.5 | 9.1 | 486.9 | 29.0 | 8.0 |

| Sample | crystal | Ns | Ni | U (ppm) | FT age (Ma) | ± | $^{206}$Pb/$^{238}$U | ± 2σ | Uncorrected ages (Ma) $^{207}$Pb / $^{235}$U | ± 2σ | $^{207}$Pb/$^{206}$Pb | ± 2σ | % discordance |
|---|---|---|---|---|---|---|---|---|---|---|---|---|---|
| | 50 | 190 | 78 | 447 | 94 | 13 | | | | | | | |
| | 51 | 162 | 17 | 78 | 361 | 92 | | | | | | | |

Note only U-Pb ages where the percentage discordance is <10 are reported. In italics are young $^{206}$Pb/$^{238}$U ages that equal the ZFT age but have a high % common Pb.

**Table 2.** Deconvoluted detrital zircon fission-track data

| Sample | Long. (°) | Lat. (°) | No. grains | Grain age distribution (Ma) Min | Max | Age dispersion $P\chi^2$ | $RE_{\%}$ | Depositional Age (Ma) | Age components (Ma) 1st (Count) | 2nd (Count) | 3rd (Count) |
|---|---|---|---|---|---|---|---|---|---|---|---|
| LS1 | 120.891 | 22.085 | 36 | 8.2 | 412.5 | 0.0 | 67.8 | 11-10 | 8.1 (1) | 113 (23) | 257 (12) |
| LS3 | 120.865 | 21.995 | 61 | 53.5 | 398.9 | 0.0 | 32.2 | 12-11 | 61 (6) | 116 (48) | 282 (7) |
| LL1 | 120.709 | 22.144 | 25 | 11.5 | 302.8 | 0.0 | 76.5 | 11-6 | 14.8 (3) | 80 (13) | 157 (9) |
| LL2 | 120.710 | 22.145 | 51 | 64.4 | 556.4 | 0.0 | 43.2 | 11-6 | 107 (17) | 239 (34) | |

LS= Loshui; LL= Lilongshan; Zeta = 127±5

**Table 3**

Key tectonic events in the evolution of south-east China

| *Event* | *Period (Ma)* | *Timing* |
|---|---|---|
| Late Yenshanian | 142-67 | Cretaceous |
| Early Yenshanian | 180-145 | Jurassic |
| Indosinian | 250-200 | Triassic |
| Caledonian | 500-400 | Ordovician-Devonian |
| Jinningian | 980-770 | Neo-proterozoic |
| Luliangian | 2000-1800 | Proterozoic |

Sources: Jahn et al., 1990; Wang et al., 2005; Wong et al., 2009.

**Table 4**

Key magmatic occurrences in the region of Taiwan from Cretaceous to present.

| *Source* | *Formation age (Ma)* |
|---|---|
| Intraplate Chiaopanshan stage | 13 - 9 |
| Luzon arc | 29 - present |
| Magmatism, northern Taiwan | 23 ± 2 |
| Intraplate Kungkuan stage | 23 - 20 |
| Oceanic crust, South China Sea | 37 - 15 |
| Huayu (Penghu Islands) | 61 - 65 |
| Tananao Complex, arc magmatism | 97 - 77 |
| Oceanic crust, eastern Taiwan | < 131 |

Sources: Richard et al., 1986; Chung et al., 1995; Deschamps et al., 2000; Chen et al., 2001; Hsu et al., 2004; Chen et al., 2010.

Data repository item 2.

**Table DR1.** Detrital zircon fission-track age data for samples from Lilongshan and Loshui

***Lilongshan: LL1***

| | |
|---|---|
| Longitude (°): | 22.1448 |
| Latitude (°): | 120.7099 |
| Stratigraphic age (Ma): | 11-6 |
| Effective track density for fluence monitor (tracks/cm^2): | 6.14E+05 |
| Relative error (%): | 3.94E-02 |
| Effective uranium content of monitor (ppm): | 39 |
| zeta factor & standard error (yr cm^2): | 127 5 |
| Size of counter square (cm^2): | 1.39E-06 |

| crystal | Ng | Ns | Ni | rho-s ($tr/cm^2$) | rho-i ($tr/cm^2$) | U (ppm) | age (Ma) | ± |
|---|---|---|---|---|---|---|---|---|
| 1 | 6 | 145 | 40 | 1.74E+07 | 4.81E+06 | 305.32 | 139.90 | 25.08 |
| 2 | 8 | 184 | 27 | 1.66E+07 | 2.44E+06 | 154.57 | 260.54 | 53.84 |
| 3 | 10 | 45 | 136 | 3.25E+06 | 9.81E+06 | 622.86 | 12.90 | 2.23 |
| 4 | 9 | 119 | 37 | 9.54E+06 | 2.97E+06 | 188.28 | 124.27 | 23.47 |
| 5 | 12 | 196 | 125 | 1.18E+07 | 7.52E+06 | 477.07 | 60.89 | 7.03 |
| 6 | 8 | 167 | 65 | 1.51E+07 | 5.86E+06 | 372.11 | 99.47 | 14.62 |
| 7 | 10 | 118 | 45 | 8.51E+06 | 3.25E+06 | 206.09 | 101.50 | 17.85 |
| 8 | 10 | 161 | 83 | 1.16E+07 | 5.99E+06 | 380.13 | 75.24 | 10.23 |
| 9 | 10 | 166 | 99 | 1.20E+07 | 7.14E+06 | 453.40 | 65.09 | 8.33 |
| 10 | 12 | 246 | 108 | 1.48E+07 | 6.49E+06 | 412.19 | 88.26 | 10.28 |
| 11 | 10 | 191 | 81 | 1.38E+07 | 5.84E+06 | 370.97 | 91.35 | 12.19 |
| 12 | 10 | 262 | 58 | 1.89E+07 | 4.18E+06 | 265.63 | 173.87 | 25.37 |
| 13 | 10 | 200 | 69 | 1.44E+07 | 4.98E+06 | 316.01 | 112.10 | 15.75 |
| 14 | 14 | 250 | 206 | 1.29E+07 | 1.06E+07 | 673.89 | 47.17 | 4.50 |
| 15 | 10 | 152 | 34 | 1.10E+07 | 2.45E+06 | 155.71 | 172.10 | 32.76 |
| 16 | 20 | 130 | 289 | 4.69E+06 | 1.04E+07 | 661.79 | 17.53 | 1.87 |
| 17 | 8 | 155 | 59 | 1.40E+07 | 5.32E+06 | 337.76 | 101.69 | 15.63 |
| 18 | 10 | 272 | 87 | 1.96E+07 | 6.28E+06 | 398.45 | 120.84 | 15.00 |
| 19 | 12 | 47 | 161 | 2.83E+06 | 9.68E+06 | 614.46 | 11.38 | 1.89 |
| 20 | 10 | 157 | 62 | 1.13E+07 | 4.47E+06 | 283.95 | 98.05 | 14.78 |
| 21 | 6 | 111 | 40 | 1.33E+07 | 4.81E+06 | 305.32 | 107.37 | 19.87 |
| 22 | 8 | 134 | 35 | 1.21E+07 | 3.16E+06 | 200.37 | 147.67 | 28.12 |
| 23 | 12 | 186 | 23 | 1.12E+07 | 1.38E+06 | 87.78 | 308.03 | 68.25 |
| 24 | 12 | 33 | 16 | 1.98E+06 | 9.62E+05 | 61.06 | 79.97 | 24.39 |
| 25 | 16 | 326 | 132 | 1.47E+07 | 5.95E+06 | 377.84 | 95.64 | 9.98 |

**Lilongshan**: ***LL2***

| | |
|---|---|
| Longitude (°): | 22.1447 |
| Latitude (°): | 120.7089 |
| Stratigraphic age: | 11-6 |
| Effective track density for fluence monitor (tracks/cm^2): | 6.14E+05 |
| Relative error (%): | 3.94E-02 |
| Effective uranium content of monitor (ppm): | 39 |
| zeta factor & standard error (yr cm^2): | 127 5 |
| Size of counter square (cm^2): | 1.39E-06 |

| crystal | Ng | Ns | Ni | rho-s ($tr/cm^2$) | rho-i ($tr/cm^2$) | U (ppm) | age (Ma) | ± |
|---|---|---|---|---|---|---|---|---|
| 1 | 8 | 191 | 76 | 1.72E+07 | 6.85E+06 | 435.08 | 97.31 | 13.28 |
| 2 | 6 | 97 | 14 | 1.17E+07 | 1.68E+06 | 106.86 | 264.80 | 75.81 |
| 3 | 20 | 128 | 18 | 4.62E+06 | 6.49E+05 | 41.22 | 271.63 | 68.50 |
| 4 | 20 | 150 | 26 | 5.41E+06 | 9.38E+05 | 59.54 | 221.24 | 47.12 |
| 5 | 12 | 60 | 10 | 3.61E+06 | 6.01E+05 | 38.17 | 229.94 | 78.62 |
| 6 | 12 | 286 | 37 | 1.72E+07 | 2.22E+06 | 141.21 | 294.73 | 51.69 |
| 7 | 14 | 244 | 72 | 1.26E+07 | 3.71E+06 | 235.53 | 130.88 | 17.67 |
| 8 | 8 | 124 | 39 | 1.12E+07 | 3.52E+06 | 223.27 | 122.87 | 22.64 |

| | | | | | | | | |
|---|---|---|---|---|---|---|---|---|
| 9 | 8 | 150 | 40 | 1.35E+07 | 3.61E+06 | 228.99 | 144.67 | 25.84 |
| 10 | 10 | 137 | 25 | 9.88E+06 | 1.80E+06 | 114.50 | 210.33 | 45.86 |
| 11 | 8 | 59 | 13 | 5.32E+06 | 1.17E+06 | 74.42 | 174.68 | 53.59 |
| 12 | 10 | 152 | 27 | 1.10E+07 | 1.95E+06 | 123.66 | 215.98 | 45.23 |
| 13 | 8 | 192 | 24 | 1.73E+07 | 2.16E+06 | 137.40 | 304.79 | 66.16 |
| 14 | 8 | 169 | 70 | 1.52E+07 | 6.31E+06 | 400.74 | 93.51 | 13.37 |
| 15 | 8 | 170 | 80 | 1.53E+07 | 7.22E+06 | 457.98 | 82.38 | 11.24 |
| 16 | 5 | 149 | 21 | 2.15E+07 | 3.03E+06 | 192.35 | 271.04 | 63.31 |
| 17 | 8 | 175 | 18 | 1.58E+07 | 1.62E+06 | 103.05 | 368.57 | 91.41 |
| 18 | 10 | 157 | 43 | 1.13E+07 | 3.10E+06 | 196.93 | 140.90 | 24.35 |
| 19 | 10 | 158 | 34 | 1.14E+07 | 2.45E+06 | 155.71 | 178.80 | 33.91 |
| 20 | 6 | 74 | 23 | 8.90E+06 | 2.77E+06 | 175.56 | 124.32 | 29.74 |
| 21 | 7 | 187 | 43 | 1.93E+07 | 4.43E+06 | 281.33 | 167.47 | 28.44 |
| 22 | 5 | 62 | 14 | 8.95E+06 | 2.02E+06 | 128.24 | 170.50 | 50.52 |
| 23 | 6 | 175 | 31 | 2.10E+07 | 3.73E+06 | 236.62 | 216.56 | 42.33 |
| 24 | 10 | 153 | 29 | 1.10E+07 | 2.09E+06 | 132.82 | 202.62 | 41.15 |
| 25 | 14 | 237 | 45 | 1.22E+07 | 2.32E+06 | 147.21 | 202.27 | 33.04 |
| 26 | 6 | 139 | 23 | 1.67E+07 | 2.77E+06 | 175.56 | 231.57 | 52.25 |
| 27 | 7 | 150 | 53 | 1.55E+07 | 5.46E+06 | 346.76 | 109.48 | 17.58 |
| 28 | 6 | 135 | 35 | 1.62E+07 | 4.21E+06 | 267.16 | 148.75 | 28.31 |
| 29 | 6 | 192 | 21 | 2.31E+07 | 2.53E+06 | 160.29 | 347.18 | 79.97 |
| 30 | 12 | 434 | 178 | 2.61E+07 | 1.07E+07 | 679.34 | 94.43 | 8.53 |
| 31 | 9 | 125 | 48 | 1.00E+07 | 3.85E+06 | 244.26 | 100.81 | 17.19 |
| 32 | 7 | 86 | 18 | 8.86E+06 | 1.86E+06 | 117.77 | 183.76 | 47.71 |
| 33 | 6 | 140 | 22 | 1.68E+07 | 2.65E+06 | 167.93 | 243.61 | 55.99 |
| 34 | 8 | 73 | 6 | 6.58E+06 | 5.41E+05 | 34.35 | 458.01 | 194.64 |
| 35 | 10 | 177 | 30 | 1.28E+07 | 2.16E+06 | 137.40 | 226.17 | 44.79 |
| 36 | 8 | 183 | 110 | 1.65E+07 | 9.92E+06 | 629.73 | 64.58 | 7.85 |
| 37 | 8 | 167 | 39 | 1.51E+07 | 3.52E+06 | 223.27 | 164.93 | 29.44 |
| 38 | 10 | 179 | 28 | 1.29E+07 | 2.02E+06 | 128.24 | 244.71 | 49.87 |
| 39 | 10 | 187 | 50 | 1.35E+07 | 3.61E+06 | 228.99 | 144.29 | 23.08 |
| 40 | 8 | 126 | 29 | 1.14E+07 | 2.62E+06 | 166.02 | 167.32 | 34.56 |
| 41 | 6 | 130 | 41 | 1.56E+07 | 4.93E+06 | 312.96 | 122.53 | 22.03 |
| 42 | 10 | 229 | 32 | 1.65E+07 | 2.31E+06 | 146.55 | 273.32 | 51.75 |
| 43 | 6 | 196 | 21 | 2.36E+07 | 2.53E+06 | 160.29 | 354.22 | 81.51 |
| 44 | 8 | 242 | 38 | 2.18E+07 | 3.43E+06 | 217.54 | 243.79 | 42.70 |
| 45 | 6 | 159 | 33 | 1.91E+07 | 3.97E+06 | 251.89 | 185.29 | 35.56 |
| 46 | 12 | 217 | 30 | 1.30E+07 | 1.80E+06 | 114.50 | 276.20 | 53.97 |
| 47 | 10 | 156 | 10 | 1.13E+07 | 7.22E+05 | 45.80 | 581.58 | 189.93 |
| 48 | 10 | 203 | 33 | 1.46E+07 | 2.38E+06 | 151.13 | 235.64 | 44.38 |
| 49 | 10 | 201 | 55 | 1.45E+07 | 3.97E+06 | 251.89 | 141.03 | 21.57 |
| 50 | 8 | 190 | 78 | 1.71E+07 | 7.03E+06 | 446.53 | 94.34 | 12.77 |
| 51 | 10 | 162 | 17 | 1.17E+07 | 1.23E+06 | 77.86 | 361.46 | 92.32 |

***LS1***

| | |
|---|---|
| Longitude (°): | 22.0849 |
| Latitude (°): | 120.8906 |
| Stratigraphic age: | 11-10 |
| Effective track density for fluence monitor (tracks/cm^2): | 6.14E+05 |
| Relative error (%): | 3.94E-02 |
| Effective uranium content of monitor (ppm): | 39 |
| zeta factor & standard error (yr cm^2): | 127 5 |
| Size of counter square (cm^2): | 1.39E-06 |

| crystal | Ng | Ns | Ni | rho-s ($tr/cm^2$) | rho-i ($tr/cm^2$) | U (ppm) | age (Ma) | ± |
|---|---|---|---|---|---|---|---|---|
| 1 | 8 | 244 | 31 | 2.20E+07 | 2.80E+06 | 177.47 | 299.99 | 57.38 |
| 2 | 6 | 153 | 38 | 1.84E+07 | 4.57E+06 | 290.06 | 155.20 | 28.23 |
| 3 | 8 | 150 | 58 | 1.35E+07 | 5.23E+06 | 332.04 | 100.12 | 15.56 |
| 4 | 6 | 80 | 16 | 9.62E+06 | 1.92E+06 | 122.13 | 192.18 | 52.71 |
| 5 | 12 | 98 | 48 | 5.89E+06 | 2.89E+06 | 183.19 | 79.17 | 14.00 |

| | | | | | | | | |
|---|---|---|---|---|---|---|---|---|
| 6 | 6 | 147 | 13 | 1.77E+07 | 1.56E+06 | 99.23 | 426.72 | 123.65 |
| 7 | 10 | 138 | 60 | 9.96E+06 | 4.33E+06 | 274.79 | 89.11 | 13.85 |
| 8 | 8 | 182 | 50 | 1.64E+07 | 4.51E+06 | 286.24 | 140.47 | 22.53 |
| 9 | 8 | 43 | 27 | 3.88E+06 | 2.44E+06 | 154.57 | 61.84 | 15.21 |
| 10 | 6 | 149 | 54 | 1.79E+07 | 6.49E+06 | 412.19 | 106.76 | 17.04 |
| 11 | 12 | 304 | 31 | 1.83E+07 | 1.86E+06 | 118.31 | 371.67 | 70.31 |
| 12 | 12 | 184 | 32 | 1.11E+07 | 1.92E+06 | 122.13 | 220.52 | 42.37 |
| 13 | 8 | 164 | 24 | 1.48E+07 | 2.16E+06 | 137.40 | 261.23 | 57.23 |
| 14 | 6 | 103 | 32 | 1.24E+07 | 3.85E+06 | 244.26 | 124.37 | 25.24 |
| 15 | 6 | 130 | 36 | 1.56E+07 | 4.33E+06 | 274.79 | 139.37 | 26.33 |
| 16 | 10 | 111 | 59 | 8.01E+06 | 4.26E+06 | 270.21 | 72.99 | 11.81 |
| 17 | 8 | 160 | 27 | 1.44E+07 | 2.44E+06 | 154.57 | 227.15 | 47.39 |
| 18 | 8 | 123 | 45 | 1.11E+07 | 4.06E+06 | 257.62 | 105.77 | 18.50 |
| 19 | 10 | 117 | 32 | 8.44E+06 | 2.31E+06 | 146.55 | 141.09 | 28.23 |
| 20 | 6 | 82 | 40 | 9.86E+06 | 4.81E+06 | 305.32 | 79.49 | 15.38 |
| 21 | 6 | 106 | 41 | 1.27E+07 | 4.93E+06 | 312.96 | 100.09 | 18.47 |
| 22 | 8 | 139 | 25 | 1.25E+07 | 2.25E+06 | 143.12 | 213.35 | 46.46 |
| 23 | 10 | 31 | 149 | 2.24E+06 | 1.08E+07 | 682.40 | 8.11 | 1.61 |
| 24 | 8 | 96 | 26 | 8.66E+06 | 2.34E+06 | 148.84 | 142.47 | 31.57 |
| 25 | 10 | 224 | 75 | 1.62E+07 | 5.41E+06 | 343.49 | 115.48 | 15.51 |
| 26 | 10 | 130 | 35 | 9.38E+06 | 2.53E+06 | 160.29 | 143.31 | 27.38 |
| 27 | 8 | 122 | 45 | 1.10E+07 | 4.06E+06 | 257.62 | 104.91 | 18.37 |
| 28 | 10 | 134 | 33 | 9.67E+06 | 2.38E+06 | 151.13 | 156.51 | 30.51 |
| 29 | 18 | 176 | 54 | 7.05E+06 | 2.16E+06 | 137.40 | 125.92 | 19.68 |
| 30 | 8 | 90 | 33 | 8.12E+06 | 2.98E+06 | 188.92 | 105.53 | 21.54 |
| 31 | 8 | 96 | 19 | 8.66E+06 | 1.71E+06 | 108.77 | 194.17 | 48.85 |
| 32 | 8 | 132 | 13 | 1.19E+07 | 1.17E+06 | 74.42 | 384.45 | 111.91 |
| 33 | 6 | 113 | 21 | 1.36E+07 | 2.53E+06 | 160.29 | 206.59 | 49.19 |
| 34 | 8 | 69 | 24 | 6.22E+06 | 2.16E+06 | 137.40 | 111.20 | 26.41 |
| 35 | 6 | 116 | 24 | 1.39E+07 | 2.89E+06 | 183.19 | 185.86 | 41.78 |
| 36 | 8 | 113 | 24 | 1.02E+07 | 2.16E+06 | 137.40 | 181.12 | 40.80 |

***LS3***

| | |
|---|---|
| Longitude (°): | 21.9952 |
| Latitude (°): | 120.8650 |
| Stratigraphic age: | 12-11 |
| Effective track density for fluence monitor (tracks/cm^2): | 6.14E+05 |
| Relative error (%): | 3.94E-02 |
| Effective uranium content of monitor (ppm): | 39 |
| zeta factor & standard error (yr cm^2): | 127 5 |
| Size of counter square (cm^2): | 1.39E-06 |

| crystal | Ng | Ns | Ni | rho-s ($tr/cm^2$) | rho-i ($tr/cm^2$) | U (ppm) | age (Ma) | ± |
|---|---|---|---|---|---|---|---|---|
| 1 | 12 | 96 | 42 | 5.77E+06 | 2.53E+06 | 160.29 | 88.56 | 16.44 |
| 2 | 12 | 75 | 30 | 4.51E+06 | 1.80E+06 | 114.50 | 96.81 | 20.96 |
| 3 | 7 | 110 | 45 | 1.13E+07 | 4.64E+06 | 294.42 | 94.67 | 16.82 |
| 4 | 8 | 105 | 33 | 9.47E+06 | 2.98E+06 | 188.92 | 122.96 | 24.61 |
| 5 | 6 | 131 | 56 | 1.58E+07 | 6.73E+06 | 427.45 | 90.63 | 14.54 |
| 6 | 10 | 180 | 65 | 1.30E+07 | 4.69E+06 | 297.69 | 107.14 | 15.59 |
| 7 | 10 | 61 | 24 | 4.40E+06 | 1.73E+06 | 109.92 | 98.41 | 23.76 |
| 8 | 8 | 163 | 33 | 1.47E+07 | 2.98E+06 | 188.92 | 189.88 | 36.36 |
| 9 | 8 | 52 | 18 | 4.69E+06 | 1.62E+06 | 103.05 | 111.73 | 30.60 |
| 10 | 8 | 145 | 43 | 1.31E+07 | 3.88E+06 | 246.17 | 130.24 | 22.70 |
| 11 | 8 | 109 | 35 | 9.83E+06 | 3.16E+06 | 200.37 | 120.37 | 23.46 |
| 12 | 9 | 94 | 32 | 7.54E+06 | 2.57E+06 | 162.84 | 113.60 | 23.31 |
| 13 | 8 | 126 | 50 | 1.14E+07 | 4.51E+06 | 286.24 | 97.57 | 16.38 |
| 14 | 10 | 103 | 30 | 7.43E+06 | 2.16E+06 | 137.40 | 132.58 | 27.58 |
| 15 | 6 | 147 | 30 | 1.77E+07 | 3.61E+06 | 228.99 | 188.39 | 37.85 |
| 16 | 6 | 74 | 13 | 8.90E+06 | 1.56E+06 | 99.23 | 218.34 | 65.75 |
| 17 | 12 | 153 | 40 | 9.20E+06 | 2.41E+06 | 152.66 | 147.53 | 26.30 |

| | | | | | | | | |
|---|---|---|---|---|---|---|---|---|
| 18 | 12 | 186 | 72 | 1.12E+07 | 4.33E+06 | 274.79 | 100.01 | 13.97 |
| 19 | 10 | 110 | 37 | 7.94E+06 | 2.67E+06 | 169.45 | 114.96 | 21.92 |
| 20 | 12 | 68 | 11 | 4.09E+06 | 6.61E+05 | 41.98 | 236.78 | 77.03 |
| 21 | 8 | 64 | 34 | 5.77E+06 | 3.07E+06 | 194.64 | 73.02 | 15.54 |
| 22 | 8 | 85 | 39 | 7.67E+06 | 3.52E+06 | 223.27 | 84.48 | 16.39 |
| 23 | 10 | 156 | 23 | 1.13E+07 | 1.66E+06 | 105.34 | 259.33 | 58.06 |
| 24 | 10 | 139 | 46 | 1.00E+07 | 3.32E+06 | 210.67 | 116.83 | 19.95 |
| 25 | 6 | 122 | 34 | 1.47E+07 | 4.09E+06 | 259.52 | 138.49 | 26.94 |
| 26 | 18 | 68 | 23 | 2.73E+06 | 9.22E+05 | 58.52 | 114.33 | 27.63 |
| 27 | 8 | 55 | 25 | 4.96E+06 | 2.25E+06 | 143.12 | 85.27 | 20.61 |
| 28 | 8 | 93 | 30 | 8.39E+06 | 2.71E+06 | 171.74 | 119.82 | 25.23 |
| 29 | 6 | 66 | 16 | 7.94E+06 | 1.92E+06 | 122.13 | 158.96 | 44.36 |
| 30 | 6 | 105 | 38 | 1.26E+07 | 4.57E+06 | 290.06 | 106.91 | 20.31 |
| 31 | 6 | 62 | 19 | 7.46E+06 | 2.28E+06 | 145.03 | 126.07 | 33.11 |
| 32 | 6 | 99 | 32 | 1.19E+07 | 3.85E+06 | 244.26 | 119.58 | 24.39 |
| 33 | 9 | 147 | 50 | 1.18E+07 | 4.01E+06 | 254.44 | 113.69 | 18.69 |
| 34 | 8 | 47 | 4 | 4.24E+06 | 3.61E+05 | 22.90 | 442.85 | 230.76 |
| 35 | 8 | 224 | 53 | 2.02E+07 | 4.78E+06 | 303.41 | 162.82 | 25.00 |
| 36 | 15 | 114 | 40 | 5.48E+06 | 1.92E+06 | 122.13 | 110.24 | 20.33 |
| 37 | 6 | 76 | 36 | 9.14E+06 | 4.33E+06 | 274.79 | 81.84 | 16.61 |
| 38 | 6 | 90 | 26 | 1.08E+07 | 3.13E+06 | 198.46 | 133.65 | 29.83 |
| 39 | 6 | 120 | 41 | 1.44E+07 | 4.93E+06 | 312.96 | 113.19 | 20.55 |
| 40 | 8 | 129 | 55 | 1.16E+07 | 4.96E+06 | 314.86 | 90.86 | 14.70 |
| 41 | 8 | 49 | 10 | 4.42E+06 | 9.02E+05 | 57.25 | 188.39 | 65.44 |
| 42 | 10 | 101 | 31 | 7.29E+06 | 2.24E+06 | 141.97 | 125.87 | 25.92 |
| 43 | 6 | 40 | 14 | 4.81E+06 | 1.68E+06 | 106.86 | 110.52 | 34.36 |
| 44 | 12 | 172 | 109 | 1.03E+07 | 6.55E+06 | 416.00 | 61.27 | 7.56 |
| 45 | 6 | 132 | 84 | 1.59E+07 | 1.01E+07 | 641.18 | 61.02 | 8.57 |
| 46 | 6 | 77 | 50 | 9.26E+06 | 6.01E+06 | 381.65 | 59.80 | 10.90 |
| 47 | 8 | 123 | 19 | 1.11E+07 | 1.71E+06 | 108.77 | 247.74 | 61.19 |
| 48 | 16 | 185 | 64 | 8.34E+06 | 2.89E+06 | 183.19 | 111.80 | 16.30 |
| 49 | 14 | 87 | 47 | 4.48E+06 | 2.42E+06 | 153.75 | 71.82 | 13.05 |
| 51 | 6 | 57 | 24 | 6.85E+06 | 2.89E+06 | 183.19 | 92.00 | 22.43 |
| 52 | 8 | 111 | 39 | 1.00E+07 | 3.52E+06 | 223.27 | 110.10 | 20.56 |
| 53 | 6 | 90 | 25 | 1.08E+07 | 3.01E+06 | 190.83 | 138.94 | 31.48 |
| 54 | 10 | 199 | 49 | 1.44E+07 | 3.54E+06 | 224.41 | 156.53 | 25.08 |
| 55 | 12 | 301 | 29 | 1.81E+07 | 1.74E+06 | 110.68 | 392.73 | 76.60 |
| 56 | 7 | 86 | 29 | 8.86E+06 | 2.99E+06 | 189.74 | 114.67 | 24.69 |
| 57 | 6 | 47 | 18 | 5.65E+06 | 2.16E+06 | 137.40 | 101.07 | 28.06 |
| 58 | 6 | 118 | 36 | 1.42E+07 | 4.33E+06 | 274.79 | 126.63 | 24.19 |
| 59 | 10 | 129 | 42 | 9.31E+06 | 3.03E+06 | 192.35 | 118.73 | 21.17 |
| 60 | 10 | 156 | 113 | 1.13E+07 | 8.15E+06 | 517.52 | 53.64 | 6.68 |
| 61 | 6 | 64 | 6 | 7.70E+06 | 7.22E+05 | 45.80 | 403.27 | 172.29 |
| 62 | 6 | 99 | 34 | 1.19E+07 | 4.09E+06 | 259.52 | 112.61 | 22.45 |

Data repository item 3.

**Table DR2.** Detrital U-Pb age data for samples from Lilongshan and Loshui

| Sample | Grain | U (ppm) | Th/U | % Com Pb | $^{206}Pb/^{238}U$ | 2 σ | $^{207}Pb/^{235}U$ | 2 σ | $^{207}Pb/^{206}Pb$ | 2 σ |
|---|---|---|---|---|---|---|---|---|---|---|
| LL1 | G1 | 630 | 0.50 | 1.23 | 226.1 | 5.4 | 234.5 | 8.5 | 306.8 | 28.8 |
| | G2 | 303 | 0.31 | 1.63 | 227.1 | 5.7 | 247.1 | 12.3 | 480.7 | 38.3 |
| | G3 | 593 | 0.44 | 6.59 | 12.2 | 3.3 | 28.3 | 4.0 | | |
| | G4 | 409 | 0.41 | 0.65 | 183.4 | 4.9 | 187.0 | 8.6 | 199.6 | 39.1 |
| | G5 | 561 | 0.35 | 0.64 | 1755.6 | 34.9 | 1809.0 | 82.5 | 1881.5 | 11.4 |
| | G6 | 106 | 0.42 | 1.24 | 138.8 | 5.2 | 146.1 | 13.4 | 491.9 | 82.5 |
| | G8 | 531 | 0.20 | 0.51 | 1686.7 | 33.6 | 1772.3 | 82.7 | 1883.8 | 11.9 |
| | G9 | 364 | 0.05 | 0.70 | 1600.8 | 31.9 | 1716.4 | 85.5 | 1902.4 | 12.3 |
| | G10 | 253 | 1.00 | 1.82 | 133.7 | 4.4 | 147.5 | 8.6 | 465.4 | 50.1 |
| | G11 | 383 | 0.47 | 0.90 | 233.4 | 5.7 | 236.6 | 10.8 | 333.1 | 36.4 |

| | | | | | | | | | | |
|---|---|---|---|---|---|---|---|---|---|---|
| | G12 | 448 | 1.11 | 3.11 | 232.0 | 5.7 | 249.2 | 11.8 | 462.2 | 36.4 |
| | G13 | 293 | 0.12 | 0.93 | 1888.7 | 38.7 | 1883.6 | 109.5 | 1916.6 | 12.5 |
| | G14 | 508 | 0.21 | 1.09 | 184.9 | 4.8 | 194.8 | 7.7 | 361.4 | 32.1 |
| | G16 | 692 | 2.14 | 2.92 | 18.9 | 3.3 | 24.5 | 3.6 | | |
| | G17 | 281 | 0.24 | 0.79 | 1906.9 | 39.5 | 1920.2 | 125.1 | 1967.3 | 12.8 |
| | G18 | 392 | 0.15 | 0.62 | 1758.3 | 36.0 | 1810.7 | 100.9 | 1873.3 | 13.0 |
| | G19 | 455 | 0.52 | 2.37 | 10.9 | 3.3 | 13.8 | 3.6 | | |
| | G21 | 242 | 0.29 | 1.02 | 193.8 | 5.2 | 196.7 | 9.4 | 319.8 | 39.7 |
| | G23 | 143 | 0.51 | 1.49 | 178.5 | 5.0 | 180.3 | 9.2 | 343.3 | 43.0 |
| | G24 | 71 | 0.45 | 2.50 | 1912.1 | 41.5 | 1820.3 | 188.2 | 1891.0 | 16.0 |
| | G25 | 262 | 0.38 | 0.62 | 173.1 | 4.9 | 169.1 | 8.5 | 190.8 | 43.5 |
| LL2 | G1 | 61 | 0.83 | -0.51 | 1976.9 | 39.1 | 1794.9 | 182.4 | 1785.9 | 15.3 |
| | G2 | 138 | 1.02 | -2.44 | 537.3 | 10.5 | 521.2 | 25.7 | 580.3 | 27.3 |
| | G3 | 108 | 0.89 | -0.94 | 1806.8 | 34.9 | 1782.9 | 155.7 | 1809.5 | 14.8 |
| | G4 | 65 | 0.82 | -0.77 | 2567.9 | 52.9 | 2358.7 | 308.2 | 2345.4 | 13.7 |
| | G5 | 46 | 0.92 | -0.65 | 980.9 | 20.7 | 891.4 | 78.4 | 998.3 | 29.4 |
| | G9 | 363 | 0.60 | -1.59 | 237.6 | 5.7 | 236.6 | 8.9 | 241.7 | 28.3 |
| | G8 | 252 | 0.67 | -1.74 | 462.6 | 9.2 | 451.7 | 18.3 | 456.7 | 25.2 |
| | G13 | 196 | 0.28 | 1.77 | 492.2 | 10.8 | 524.9 | 30.6 | 777.2 | 31.3 |
| | G16 | 355 | 0.41 | 0.60 | 259.4 | 6.8 | 263.8 | 13.7 | 328.4 | 39.6 |
| | G17 | 173 | 0.61 | 1.82 | 779.1 | 15.8 | 775.8 | 42.3 | 889.1 | 22.7 |
| | G19 | 153 | 0.50 | 1.31 | 2857.2 | 63.0 | 2790.0 | 386.8 | 2833.0 | 11.5 |
| | G21 | 481 | 0.72 | -0.11 | 227.4 | 6.1 | 247.4 | 9.7 | 518.0 | 28.9 |
| | G24 | 106 | 0.47 | 1.62 | 2415.8 | 52.1 | 2328.0 | 261.6 | 2365.1 | 12.8 |
| | G26 | 389 | 0.32 | 0.50 | 1886.9 | 39.9 | 1863.3 | 170.3 | 1831.5 | 15.3 |
| | G29 | 235 | 0.58 | 0.32 | 498.0 | 10.5 | 474.1 | 21.4 | 477.9 | 27.6 |
| | G30 | 794 | 0.18 | 1.12 | 155.6 | 5.2 | 168.8 | 6.8 | 384.3 | 28.9 |
| | G31 | 291 | 2.44 | -4.15 | 132.6 | 5.2 | 134.6 | 9.2 | 245.8 | 59.2 |
| | G33 | 361 | 0.66 | 0.78 | 172.5 | 5.6 | 176.0 | 9.2 | 290.7 | 42.7 |
| | G34 | 94 | 0.55 | 1.60 | 1841.9 | 43.9 | 1742.0 | 266.1 | 1802.7 | 23.2 |
| | G36 | 1417 | 0.20 | 0.16 | 187.5 | 5.6 | 188.1 | 7.6 | 171.1 | 31.0 |
| | G37 | 166 | 1.23 | -1.54 | 360.7 | 7.8 | 345.8 | 17.8 | 366.9 | 35.3 |
| | G39 | 373 | 0.86 | -0.28 | 240.1 | 6.4 | 240.1 | 10.5 | 287.2 | 33.7 |
| | G40 | 315 | 2.72 | -4.18 | 243.5 | 6.8 | 257.8 | 14.8 | 465.8 | 43.5 |
| | G43 | 483 | 1.00 | -0.01 | 2554.9 | 57.8 | 2525.5 | 290.6 | 2519.1 | 15.1 |
| | G44 | 363 | 0.99 | -0.38 | 251.2 | 6.6 | 258.9 | 11.2 | 358.9 | 32.6 |
| | G48 | 117 | 0.62 | 0.02 | 853.3 | 15.5 | 812.2 | 37.1 | 850.2 | 19.2 |
| | G49 | 251 | 0.93 | -0.44 | 215.7 | 5.4 | 234.5 | 9.1 | 486.9 | 29.0 |
| | G51 | 59 | 0.56 | 1.29 | 924.1 | 17.3 | 851.7 | 50.9 | 926.9 | 22.1 |
| LS1 | G1 | 127 | 0.49 | 1.50 | 446.2 | 4.3 | 444.1 | 23.3 | 626.1 | 30.5 |
| | G2 | 365 | 0.29 | 0.44 | 1839.3 | 0.8 | 1849.7 | 107.1 | 1855.2 | 11.5 |
| | G5 | 233 | 0.45 | 0.81 | 127.5 | 1.7 | 138.3 | 8.3 | 408.6 | 47.9 |
| | G6 | 37 | 0.72 | 6.12 | 2156.7 | 3.0 | 2113.9 | 409.0 | 2260.8 | 17.2 |
| | G8 | 303 | 0.80 | -0.38 | 1658.2 | 1.5 | 1735.0 | 91.9 | 1870.6 | 11.5 |
| | G10 | 357 | 0.29 | 0.31 | 1879.8 | 2.7 | 1911.9 | 132.1 | 2024.8 | 11.6 |
| | G11 | 189 | 0.47 | 0.43 | 1994.2 | 1.3 | 1933.0 | 120.9 | 1917.2 | 11.4 |
| | G12 | 234 | 0.58 | 0.08 | 1751.2 | 1.5 | 1778.3 | 107.6 | 1846.9 | 11.8 |
| | G13 | 304 | 0.38 | 0.04 | 792.5 | 1.6 | 786.8 | 32.2 | 819.6 | 17.8 |
| | G14 | 58 | 0.40 | 2.42 | 1916.8 | 2.2 | 1809.7 | 203.5 | 1883.6 | 14.8 |
| | G15 | 254 | 0.48 | 0.10 | 322.6 | 0.7 | 321.5 | 12.9 | 400.4 | 27.8 |
| | G17 | 323 | 0.53 | -0.02 | 750.8 | 1.3 | 741.6 | 32.8 | 836.8 | 19.1 |
| | G19 | 275 | 0.36 | 0.13 | 250.4 | 3.4 | 255.5 | 10.3 | 343.7 | 29.6 |
| | G22 | 130 | 0.51 | 0.14 | 1713.2 | 1.8 | 1629.9 | 126.5 | 1666.1 | 13.9 |
| | G24 | 99 | 0.63 | 1.88 | 805.9 | 0.7 | 850.5 | 53.6 | 1152.0 | 22.0 |
| | G25 | 307 | 0.39 | 0.23 | 2227.6 | 1.5 | 2231.6 | 147.0 | 2261.4 | 10.7 |
| | G26 | 191 | 0.85 | -0.12 | 135.1 | 0.7 | 130.6 | 7.7 | 163.5 | 49.0 |
| | G27 | 337 | 0.24 | 0.22 | 1758.3 | 1.0 | 1759.8 | 95.6 | 1841.3 | 11.6 |
| | G28 | 188 | 0.48 | 1.06 | 149.4 | 1.2 | 155.1 | 8.6 | 356.8 | 44.8 |
| | G29 | 142 | 0.62 | 1.11 | 113.2 | 2.1 | 106.5 | 7.3 | 116.9 | 57.7 |
| | G30 | 207 | 0.71 | 1.25 | 138.2 | 0.9 | 148.5 | 8.9 | 357.6 | 48.5 |
| | G31 | 76 | 0.50 | 1.57 | 289.1 | 2.8 | 305.3 | 20.8 | 580.7 | 47.0 |
| | G32 | 98 | 0.74 | 1.30 | 846.1 | 2.8 | 828.5 | 44.7 | 943.2 | 20.5 |
| | G33 | 154 | 0.29 | 0.81 | 223.8 | 0.7 | 225.1 | 10.9 | 358.9 | 37.2 |
| | G35 | 347 | 0.41 | 0.44 | 1969.6 | 3.8 | 1936.1 | 106.0 | 1879.7 | 11.2 |
| LS3 | G1 | 146 | 1.01 | 1.32 | 127.5 | 5.6 | 123.8 | 11.0 | 138.7 | 82.4 |
| | G2 | 125 | 0.61 | 1.39 | 139.5 | 5.8 | 136.9 | 11.5 | 238.1 | 76.2 |
| | G5 | 940 | 0.43 | 1.02 | 2227.1 | 46.0 | 2314.6 | 138.8 | 2365.0 | 11.5 |
| | G8 | 170 | 0.37 | 1.53 | 823.6 | 16.9 | 825.6 | 49.5 | 919.2 | 23.5 |
| | G9 | 136 | 0.61 | 1.57 | 128.9 | 5.8 | 127.9 | 11.8 | 229.5 | 84.3 |
| | G10 | 430 | 0.77 | 1.93 | 133.2 | 5.3 | 153.3 | 8.1 | 551.9 | 39.4 |
| | G12 | 163 | 1.28 | 2.05 | 136.0 | 5.7 | 151.6 | 11.7 | 469.7 | 66.0 |
| | G14 | 144 | 0.45 | 0.53 | 174.4 | 6.0 | 173.9 | 11.6 | 299.0 | 56.9 |
| | G16 | 129 | 0.61 | 1.31 | 1760.8 | 35.4 | 1686.8 | 122.7 | 1757.3 | 13.9 |
| | G17 | 142 | 0.64 | 0.36 | 278.2 | 7.3 | 256.6 | 14.4 | 276.1 | 44.0 |
| | G21 | 172 | 0.50 | 0.70 | 120.8 | 5.3 | 121.7 | 8.8 | 341.6 | 61.3 |
| | G23 | 121 | 0.46 | 0.70 | 269.4 | 7.3 | 258.5 | 15.9 | 356.4 | 47.8 |
| | G24 | 392 | 1.29 | -1.89 | 141.2 | 5.4 | 142.6 | 7.6 | 257.5 | 41.0 |

| | | | | | | | | | |
|---|---|---|---|---|---|---|---|---|---|
| G25 | 238 | 0.66 | 0.27 | 196.0 | 6.3 | 201.0 | 13.7 | 318.1 | 56.2 |
| G26 | 50 | 0.91 | 0.53 | 150.0 | 6.3 | 146.7 | 15.3 | 396.3 | 95.8 |
| G27 | 89 | 0.68 | 2.94 | 135.2 | 6.4 | 139.5 | 16.6 | 494.2 | 107.9 |
| G28 | 195 | 0.42 | 0.54 | 174.3 | 5.8 | 176.9 | 9.7 | 306.4 | 44.1 |
| G31 | 208 | 0.58 | 0.56 | 247.6 | 6.9 | 262.5 | 14.0 | 472.1 | 40.2 |
| G32 | 281 | 0.72 | 0.48 | 178.9 | 5.8 | 196.8 | 9.4 | 503.5 | 36.0 |
| G35 | 458 | 0.24 | 0.75 | 1530.9 | 31.0 | 1654.0 | 86.2 | 1854.9 | 13.5 |
| G39 | 341 | 0.61 | 0.46 | 241.6 | 6.7 | 244.4 | 11.8 | 300.3 | 37.3 |
| G40 | 576 | 0.53 | -0.08 | 184.4 | 5.8 | 185.6 | 8.1 | 267.7 | 32.8 |
| G41 | 138 | 1.45 | 0.47 | 246.6 | 7.3 | 241.4 | 16.0 | 385.2 | 52.3 |
| G42 | 136 | 0.90 | 0.39 | 252.0 | 7.5 | 253.2 | 17.9 | 377.7 | 55.4 |
| G45 | 596 | 0.28 | 0.67 | 2203.4 | 46.7 | 2194.3 | 144.8 | 2216.7 | 12.8 |
| G46 | 451 | 0.63 | 0.63 | 131.8 | 5.4 | 134.5 | 7.6 | 213.9 | 44.3 |
| G47 | 114 | 1.11 | 1.29 | 846.0 | 17.7 | 785.0 | 43.7 | 804.8 | 23.9 |
| G48 | 193 | 1.14 | 0.22 | 241.0 | 6.7 | 238.3 | 11.6 | 318.1 | 37.8 |
| G50 | 249 | 0.44 | 1.81 | 138.9 | 5.6 | 143.1 | 9.9 | 268.6 | 58.4 |
| G51 | 206 | 0.81 | 1.14 | 133.9 | 5.5 | 137.9 | 8.9 | 321.5 | 53.1 |
| G52 | 395 | 0.66 | 1.06 | 236.1 | 6.6 | 237.6 | 10.4 | 297.7 | 33.1 |
| G53 | 246 | 0.26 | 0.49 | 1967.5 | 43.4 | 1915.0 | 205.9 | 1882.9 | 16.6 |